Original Article

Avicenna Journal of Medical Biotechnology
Volume 18, Issue 4, 294-317
https://doi.org/10.18502/ajmb.v18i4.22927

Check for updates

Transcriptomic Analysis of EpCAM/CD45 Dual-Positive Ovarian Cancer Stem-Like Cells Reveals Inflammatory Signatures and Association with SYK

Mohammad Reza Tayebizadeh-Meigooni, Mahboubeh Safari Kharkeshi, Sadra Daneshvari, and Ghamartaj Hossein *

Department of Animal Biology, Developmental Biology Group, School of Biology, College of Science, University of Tehran, Tehran, Iran

Abstract

Background: Dual-positive EpCAM^{+}/CD45^{+} ovarian cancer cells in malignant ascites are proposed as ovarian cancer stem-like cells, yet their cellular origin and transcriptomic programs remain debated.

Methods: In this work expression data from ascites-derived EpCAM^{+}/CD45^{+} dual-positive ovarian cancer stem-like cells (DpOCSCs; GSE75036) and reference non-dual-positive ovarian cancer stem cells (OCSCs; GSE90125, GSE216627) was integrated. The workflow included cross-platform harmonization, differential expression analysis, pathway enrichment, protein–protein interaction mapping, and evaluation in independent cohorts (TCGA, CPTAC, survival databases).

Results: DpOCSCs showed 347 up-regulated and 23 down-regulated genes ($|\log_2 FC|>1$, FDR<0.1). Enrichment analyses revealed overrepresentation of interferon-α/γ responses, TNF, NF-κB, IL-6, JAK-STAT3, and CXCR4 signaling, and pathways linked to natural killer cell-mediated cytotoxicity, indicating a distinct inflammatory signature. Network analysis identified 17 up-regulated hub genes; 10 had higher mRNA in ovarian tumors versus normal tissues (TCGA), and 3 (SYK, CD74, MX1) showed elevated protein in CPTAC. In bulk ovarian cancer cohorts, these hubs were exploratorily associated with copy-number amplifications, immune-checkpoint expression, immunosuppressive infiltration, and clinicopathological features, including lymphatic/venous invasion and therapy outcomes. Survival and ROC analyses indicated context-dependent associations of SYK, CD74, and MX1 with overall and progression-free survival; SYK achieved an AUC ≈0.7 for predicting 6-month relapse, particularly in paclitaxel-treated patients. Transcription-factor enrichment implicated Wnt/β-catenin, Hippo, and NF-κB as upstream regulators.

Conclusion: These *in silico* findings are hypothesis-generating and nominate a SYK-associated inflammatory network for functional assessment in DpOCSCs and as a potential source of exploratory biomarkers for recurrent ovarian cancer.

*** Corresponding author:**
Ghamartaj Hossein, Ph.D.,
Department of Animal Biology,
Developmental Biology group,
School of Biology, College of Science, University of Tehran,
Tehran, Iran
Tel: +98 21 61112622
E-mail:
ghossein@ut.ac.ir
Received: 30 May 2026
Accepted: 20 Sept 2026

Keywords: Gene expression profiling, Interferons, Neoplastic stem cells, Ovarian neoplasms, Protein interaction mapping, Transcription factors
To cite this article: Tayebizadeh-Meigooni MR, Safari Kharkeshi M, Daneshvari S, Hossein Gh. Transcriptomic Analysis of EpCAM/CD45 Dual-Positive Ovarian Cancer Stem-Like Cells Reveals Inflammatory Signatures and Association with SYK. Avicenna J Med Biotech 2026;18(4):294-317.

Introduction

Epithelial Ovarian Cancer (EOC) is a heterogeneous group of tumors, and High-Grade Serous Ovarian Carcinoma (HGSOC) is its most common histological subtype, accounting for approximately 70% of EOC cases [1], yet five-year survival rates remain below 50% due principally to late-stage diagnoses [2]. Strong evidence implicates precursor lesions in the distal fimbriae of the fallopian tube as the origin of HGSOC [3], although the Ovarian Surface Epithelium (OSE) has also been proposed as a possible source [4]. HGSOC progression involves the development of malignant ascites and omental metastases [5], creating an ascites-rich tumor microenvironment that promotes cellular heterogeneity, chemoresistance, and recurrence [6]. Chemo-

This work is licensed under a Creative Commons Attribution–NonCommercial 4.0 International License.

Table 1. Details of OCSC-associated datasets

Dataset name	Platform	Sample size	Samples data	Age (*yrs*)	Publication
GSE75036 (Differential expression signature of EpiCAM/CD45 positive cells in ascitic fluid from serous ovarian cancer patients)	GPL10558 Illumina HumanHT-12 V4.0 expression beadchip	4 samples (2 populations of EpCAM/ CD45 dual-positive cells and 2 populations of EpCAM only positive cells)	Ascites derived-serous ovarian cancer cells	Patients median: 47 (18-65)	Akhter MZ, Sharawat SK, Kumar V, Kochat V, Equbal Z, Ramakrishnan M, *et al*. Aggressive serous epithelial ovarian cancer is potentially propagated by EpCAM(+)CD45(+) phenotype. Oncogene. 2018;37(16):2089-103
GSE90125 (Gene expression profiling of spheres from primary ovarian cancer cells and from primary fallopian tube epithelial cells)	GPL17692 [HuGene-2_1-st] Affymetrix Human Gene 2.1 ST Array	7 HGSOCs (3-5 samples in each group), 9 Fimbriae (3-5 samples in each group)	Ascites derived-HGSOC (FIGO stage IIIC) and ovarian normal fimbriae	Patients median: 55 (42-72) and Fimbriae samples median: 48 (39-67)	Lupia M, Angiolini F, Bertalot G, Freddi S, Sachsenmeier KF, Chisci E, *et al*. CD73 Regulates Stemness and Epithelial-Mesenchymal Transition in Ovarian Cancer-Initiating Cells. Stem Cell Reports. 2018;10(4):1412-25
GSE216627 (Matrix Gla Protein acts as a driver of stemness and tumor initiation in ovarian cancer)	GPL17692 [HuGene-2_1-st] Affymetrix Human Gene 2.1 ST Array	4 Samples (2 ascites derived- HGSOC OCSC and 2 ascites derived-HGSOC bulk)	Peritoneal ascites derived- HGSOC (FIGO stage IIIC)	Patients median: 55 (42-72)	Nieddu V, Melocchi V, Battistini C, Franciosa G, Lupia M, Stellato C, *et al*. Matrix Gla Protein drives stemness and tumor initiation in ovarian cancer. Cell Death Dis. 2023;14(3):220

therapy-resistant Ovarian Cancer Stem Cells (OCSCs) have been isolated from malignant ascites and are thought to possibly contribute to relapse [7,8], yet their cellular origin remains debated. Proposed mechanisms include Epithelial-to-Mesenchymal Transition (EMT) [9] and putative cell fusion between $EpCAM^+$ tumor cells and hematopoietic populations, generating EpCAM/ CD45 dual-positive hybrids [10,11]. However, it is important to note that the $EpCAM^+$/ $CD45^+$ phenotype alone does not constitute definitive proof of cell fusion; alternative explanations, such as trogocytosis, exosome-mediated marker transfer, phagocytic uptake, or flow-cytometric doublets, cannot be excluded based solely on surface-marker expression.

At present, transcriptomic and genetic features of EpCAM/CD45 Dual positive Ovarian Cancer Stem-like Cells (DpOCSCs) are incompletely defined, partly because available datasets contain only a small number of such samples. Here, the authors performed an integrated transcriptomic, network, and clinical- correlation analysis to compare DpOCSCs with reference OCSC populations, identify robust hub genes and pathways, and explored their clinical and immunological correlates in large ovarian cancer cohorts. In particular, *SYK*, *CD74*, and *MX1* as hub genes associated with the DpOCSCs were identified.

Materials and Methods

Data collection and processing

Gene expression datasets, including GSE90125, GSE216627, and GSE75036, were obtained from the NCBI GEO database. Details regarding platform, sample size, sample data, age, and related publications are presented in table 1. DpOCSC samples (n=2; GSM1941116, GSM1941118) were obtained from GSE75036, which was generated on the Illumina HumanHT-12 V4.0 Expression BeadChip platform (GPL10588). Comparator OCSC samples were obtained from GSE90125 (GSM2398960, GSM2398961) and GSE216627 (GSM6684690, GSM6684691), both generated on the Affymetrix Human Gene 2.1 ST Array platform (GPL17692). All three datasets are microarray-based human gene-expression profiling. The processed expression matrices provided by the original submitters were used. Probe identifiers were mapped to gene symbols using the corresponding platform annotation files, probes without valid gene annotations were removed, and when multiple probes mapped to the same gene, their expression values were summarized by taking the mean. To enable cross-platform integration, only genes shared across all datasets were retained prior to batch correction. Batch effects were corrected using the ComBat function in the sva package, with dataset specified as the batch variable and cell type (DpOCSC *vs*. OCSC) retained as the biological variable of interest. Sample quality was assessed using boxplots and Principal Component Analysis (PCA), and no samples were excluded after QC.

Differential gene expression analysis

Differentially Expressed Genes (DEGs) between DpOCSCs and OCSCs were identified using the Limma package. The limma pipeline with empirical Bayes moderation was applied to improve variance estimation despite the small sample size. Linear models were fitted to the normalized microarray expression data using the lmFit () function, followed by empirical Bayes moderation with the eBayes () function to improve the estimation of gene-wise variances and increase the statistical power of differential expression analysis, particularly given the relatively small sample size. Given the small number of DpOCSC samples, DEGs were defined using $|\log_2 FC|>1$ and FDR<0.1 to balance sensitivity and specificity. Volcano plots were generated using VolcaNoseR2 for visualization.

Protein-protein interaction (PPI) network and identification of hub genes

The Protein-Protein Interaction (PPI) network was constructed from the DEG-derived input gene set using the STRING database plugin in Cytoscape (version 3.10.2). The network was constructed from the DEG-derived input gene set using a confidence score cutoff of 0.4 and combined evidence selected for interaction retrieval. Hub genes were prioritized using CytoHubba (version 0.1) by applying eight centrality algorithms, including Stress, Radiality, MNC, MCC, EPC, Degree, Closeness, and Betweenness. For each algorithm, the top 50 ranked genes were extracted, and genes appearing in all eight ranked lists were defined as common hub genes. These candidates were further evaluated using CentiScape (version 2.1) to support topological prioritization.

Gene ontology and pathway enrichment analysis

Gene ontology analyses, including Biological Process (BP), Cellular Component (CC), and Molecular Function (MF), as well as MSigDB Hallmark and KEGG pathway [12] enrichment, were performed with the Enrichr database. The top ten terms for each category were selected using a significance threshold of an adjusted $p<0.05$. Additional enrichment factor analysis and visualization were performed in R (version 4.3.1).

Hub gene evaluation

Hub gene expression was supported at the mRNA level using TCGA datasets *via* GEPIA for tumor (n= 426) and normal (n=88) samples (TCGA normal and GTEx data), and at the protein level using UALCAN for tumor (n=100) and normal (n=25) samples. Expression across 33 cancer types was analyzed with GEPIA.

Association of TCGA-supported hub genes with OvCa stages and genetic alterations

Hub gene expression across ovarian cancer stages was analyzed in TCGA using GEPIA. Genetic alterations were explored using cBioPortal in five ovarian cancer datasets: High-Grade Serous Ovarian Carcinoma (MSK, NPJ Genome Medicine 2021, n=45), TCGA Firehose Legacy (n=617), TCGA Nature 2011 (n=489), TCGA PanCancer Atlas (n=585), and TCGA GDC 2025 (n=602).

Kaplan-Meier survival analysis

The impact of TCGA-supported hub genes on Overall Survival (OS) and Progression-Free Survival (PFS) was assessed with KM Plotter across multiple datasets. OS analysis included all cases of serous ovarian carcinoma (n=1207), GSE9891, GSE30161, GSE26193, GSE18520, and TCGA OvCa (n=557). PFS analysis included the same datasets, with GSE-51373 and TCGA OvCa (n=522) included as well. Cut-off values were selected using the default percentile-based setting in KM Plotter.

Assessment of predictive biomarkers

Predictive biomarkers were evaluated using Receiver Operating Characteristic (ROC) curve analysis with ROC Plotter for ovarian cancer. The analysis focused on Relapse-Free Survival (RFS) at six months (n=1,347) in three treatment conditions: any chemotherapy, platinum-based therapy, and paclitaxel. Diagnostic performance was assessed individually and in multi-gene combinations, considering an Area Under the Curve (AUC) of 0.7 or higher as acceptable. AUC values were not corrected for multiple testing and are therefore exploratory.

Correlation with immune checkpoint proteins and immune infiltrating cells

Gene expression data for ovarian serous cystadenocarcinoma from the Cancer Genome Atlas (GDC-TCGA-OV) were retrieved from the UCSC Xena database in the form of STAR-TPM normalized RNA-seq reads. Expression values were subsequently transformed using a log2 (TPM+1) conversion. Pearson correlation coefficients, along with their corresponding p-values, were computed for the selected gene pairs. To correct for multiple hypothesis testing, p-values were adjusted using the Benjamini–Hochberg False Discovery Rate (FDR) procedure. All correlation analyses and associated data visualizations were carried out in R (version 4.2.0). Additionally, the relationship between the identified hub genes and immune infiltrating cell populations within the TCGA-OV cohort was explored using the Timer 2.0 platform.

Analysis of transcriptional regulation of TCGA-supported hub genes

Transcriptional regulation was investigated for six principal signaling pathways relevant to OCSC: STAT3, TGFβ/Smad2/3/4, Hippo-YAP1/TAZ-TEAD, NF-κB, Notch/RBPJ, and Wnt/β-catenin-TCF/LEF [13]. The Enrichr transcription panel, including ChEA 2022 and ENCODE TF ChIP-seq 2015 data, was used for analysis. Additional resources considered included TRUST Transcription Factors 2019, TRANSFAC, and JASPAR position weight matrices. TF–target relationships compiled from these resources include predicted and ChIP-supported interactions and should be viewed as putative rather than experimentally confirmed in DpOCSCs.

Clinico-pathological evaluation of DpOCSCs-related hub genes

Associations between hub gene expression and clinical features, such as lymphatic and venous invasion, neoplasm histologic grade, new neoplasm event type, and therapy outcome, were evaluated using UCSC Xena Browser (TCGA OV, n=308). Gene expression was dichotomized based on a Gaussian distribution-derived cutoff, using Cut-off Finder [14], and chi-square tests were applied as appropriate. A comprehensive data table categorized patients by hub gene expression using TCGA IDs in R (version 4.3.1).

Statistical analysis

All statistical analyses were performed in R (version 4.3.1). Figures were generated using GraphPad Prism 9 and the SRplot online tool. Differential expression analysis was conducted using the limma package, and False Discovery Rate (FDR) correction was applied to control for multiple testing. Unless otherwise specified, results from exploratory downstream analyses are reported using nominal p-values and should be interpreted as hypothesis-generating. For exploratory analyses, nominal p-values are reported; however, given the hypothesis-generating nature of this study, all results should be interpreted with caution and require independent evaluation in external cohorts.

Up-regulated genes in DpOCSCs are related to inflammatory pathways

A total of 347 genes were up-regulated and 23 were down-regulated in DpOCSCs (EpCAM/CD45 dual-positive cells) compared with OCSCs, as revealed by transcriptome analysis of the GSE75036, GSE90125, and GSE216627 datasets (Figure 1A). Volcano plot and heatmap analyses showed a distinct molecular profile, with the top 10 up-regulated and top 5 down-regulated genes in DpOCSCs and OCSCs (GSM-1941116, GSM1941118; GSM2398960, GSM2398961, GSM6684690, GSM6684691) shown in figures 1B and 1C.

GO biological process enrichment analysis revealed overrepresentation of interferon-response terms, TNF, NF-κB, IL-6, JAK-STAT3, and CXCR4 chemokine signaling, as well as genes associated with reduced susceptibility to natural killer cell-mediated cytotoxicity, these terms might be interpreted as indicating an immune-evasive, cytokine-rich phenotype for DpOCSCs, along with potential innate immune dysregulation (Figure 2A). Functional studies will be required to determine whether these signatures reflect immune evasion or altered cytokine signaling at the

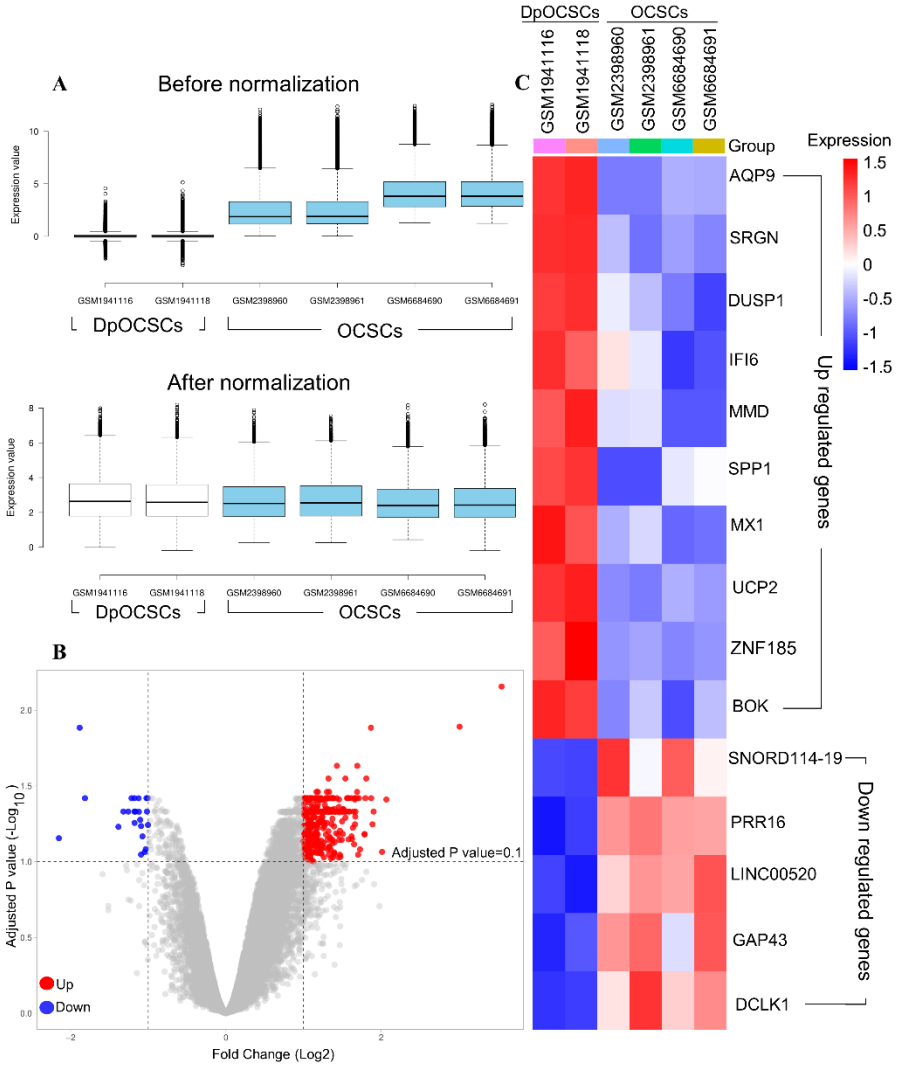

Figure 1. Differential expression profile of EpCAM/CD45 dual-positive ovarian cancer stem cells (DpOCSCs) compared with non-fused OCSCs. (A) Boxplots show expression distributions before and after batch correction for two DpOCSC samples and four OCSC samples across three GEO datasets. (B) Volcano plot of all genes with thresholds $|\log_2 FC| > 1$ and FDR <0.1; red, up-regulated in DpOCSCs; blue, down-regulated. (C) Heatmap of the top 10 up-regulated and top 5 down-regulated genes illustrates consistent expression differences between groups.

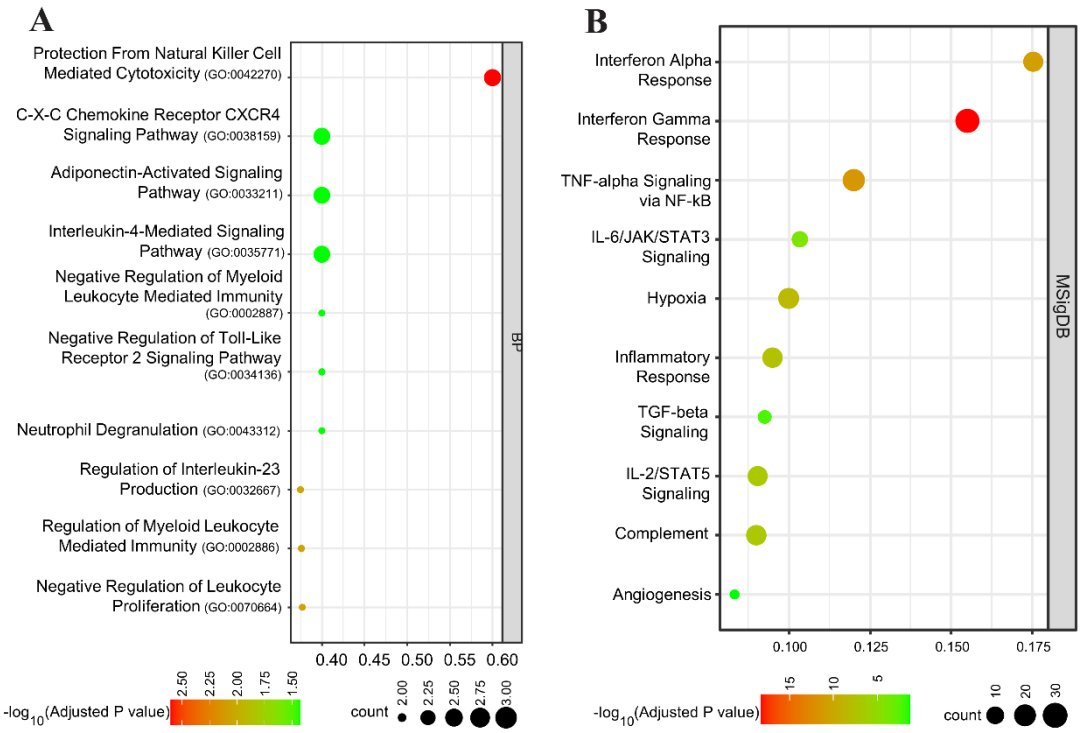

Figure 2. Functional enrichment of differentially expressed genes in DpOCSCs. (A) Bubble plot of top enriched GO biological-process terms for up-regulated genes, highlighting immune and inflammatory pathways; bubble size reflects gene count and color indicates adjusted p value. (B) Hallmark gene-set enrichment for up-regulated genes shows strong enrichment of interferon α/γ response, TNF–NF-κB, and IL-6–JAK–STAT3 signaling.

protein level. MSigDB Hallmark analysis highlighted interferon-γ and interferon-α responses as the most enriched signatures, together with TNF-α signaling *via* NF-κB, IL-6–JAK–STAT3 signaling, hypoxia, and broader inflammatory-response terms (Figure 2B). These modules are consistent with an interferon-inflamed, TNF-associated state in DpOCSCs. Down-regulated genes were mapped to fibroblast growth factor receptor signaling and cellular responses to FGF (Figure S1). The top enriched biological process terms for both up- and down-regulated gene sets, together with the top hallmark pathways for up-regulated genes, are listed in table S1. Cellular component and molecular function terms for these gene sets are provided in table S2.

PPI network and hub genes

The PPI network among Differentially Expressed Genes (DEGs) is shown in figure S2. The top 50 ranked genes from eight CytoHubba centrality algorithms were intersected, yielding 17 common hub genes that were all up-regulated in DpOCSCs. This intersection strategy was used to increase robustness and reduce algorithm-specific bias (Table S3). These analyses revealed 17 hub genes associated with DpOCSCs, and notably, every single one of them was part of the up-regulated gene set (Figure 3A). Details of the relationships among these 17 hub genes, including network connectivity and key communication points, are presented in table S4.

Gene Ontology (GO) analysis focused on ovarian cancer-relevant terms showed that these hub genes are primarily involved in processes such as chemokine and cytokine production, also immune cell activity. Terms related to macrophage activation and interleukin-6 (IL-6) and interleukin-8 (IL-8) signaling were particularly prominent (Figure 3B). Cellular component terms were frequently linked to vesicle membrane localization, and molecular function terms were predominantly related to MHC class II binding, kinase binding, and GTPase activity (Table S5).

Further KEGG and MSigDB Hallmark enrichment analysis focused on ovarian cancer-relevant terms indicated that these hub genes are associated with inflammatory and immune processes. Significant pathways included NF-κB signaling, Toll-like receptor signaling, and PD-1/PD-L1 pathway (Table 2). These results were consistent with the MSigDB findings, which showed strong enrichment of interferon-γ response, interferon-α response, TNF-α signaling *via* NF-κB, and inflammatory response terms, as detailed in table 2. Collectively, these analyses indicate that the hub genes occupy central positions in inflammatory and immune-related networks and may contribute to the DpOCSC transcriptional program, although direct

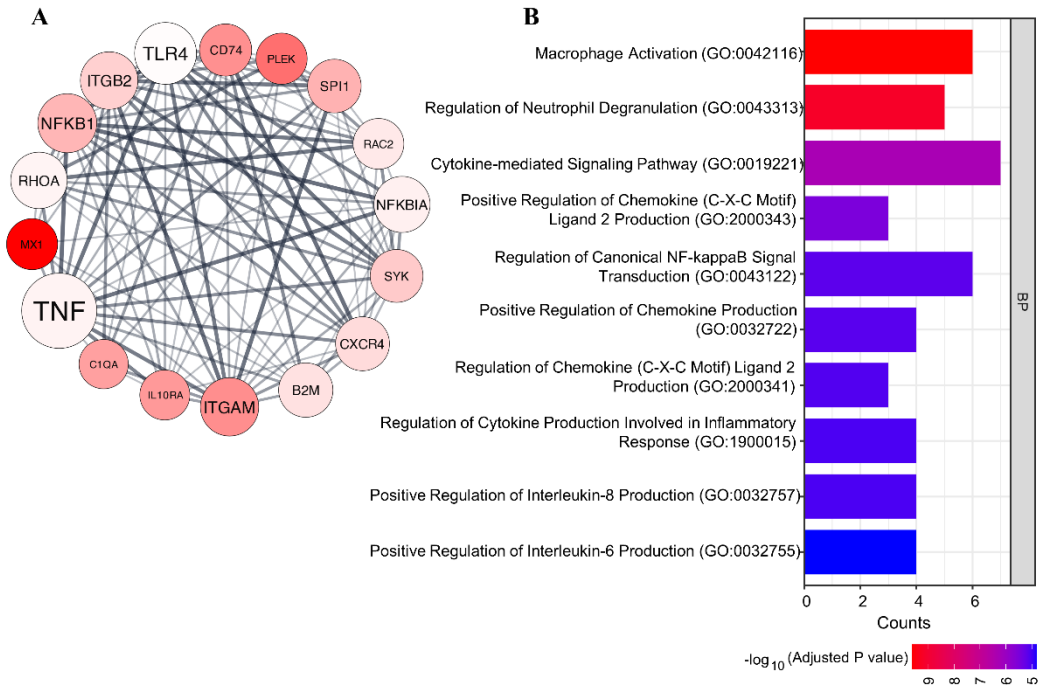

Figure 3. Identification of DpOCSCs-related hub genes using distinct algorithms and GO analysis. (A) STRING-derived Protein-Protein Interaction (PPI) network displaying the 17 hub genes. The white to red color spectrum nodes indicate Log_2FC (range 1.01-1.87), node size corresponds to the degree of each node and thickness of edges represents confidence score of interaction (>0.4). (B) Enrichment analysis of Biological Process (BP) terms for hub genes (results limited to OvCa-related terms) (adj. $p<0.05$).

Table 2. Enrichment analysis of hub genes in KEGG pathways and MSigDB Hallmark

Term	Adjusted p-value	Overlap	Genes
KEGG pathway			
Neutrophil extracellular trap formation	3.94E-08	6/159	*ITGAM; SYK; ITGB2; RAC2; TLR4; NFKB1*
NF-kappa B signaling pathway	1.81E-07	5/104	*NFKBIA; SYK; TNF; TLR4; NFKB1*
NOD-like receptor signaling pathway	2.31E-06	5/185	*NFKBIA; TNF; TLR4; RHOA; NFKB1*
Chemokine signaling pathway	2.59E-06	5/191	*NFKBIA; RAC2; CXCR4; RHOA; NFKB1*
Toll-like receptor signaling pathway	8.40E-06	4/109	*NFKBIA; TNF; TLR4; NFKB1*
Pathways in cancer	1.25E-05	6/525	*NFKBIA; SPI1; RAC2; CXCR4; RHOA; NFKB1*
Natural killer cell mediated cytotoxicity	1.54E-05	4/131	*SYK; ITGB2; RAC2; TNF*
RIG-I-like receptor signaling pathway	8.19E-05	3/71	*NFKBIA; TNF; NFKB1*
cAMP signaling pathway	8.95E-05	4/222	*NFKBIA; RAC2; RHOA; NFKB1*
PD-L1 expression and PD-1 checkpoint pathway in cancer	1.43E-04	3/88	*NFKBIA; TLR4; NFKB1*
MSigDB hallmark			
Interferon gamma response	2.20E-07	6/200	*NFKBIA; CD74; IL10RA; MX1; B2M; NFKB1*
TNF-alpha signaling *via* NF-kB	1.46E-04	4/200	*NFKBIA; PLEK; TNF; NFKB1*
Interferon alpha response	3.76E-04	3/97	*CD74; MX1; B2M*
KRAS signaling up	0.0018	3/200	*IL10RA; ITGB2; CXCR4*
Complement	0.0018	3/200	*C1QA; ITGAM; PLEK*
Inflammatory response	0.0018	3/200	*NFKBIA; IL10RA; NFKB1*
Coagulation	0.0158	2/138	*C1QA; PLEK*
Apical junction	0.0257	2/200	*SYK; RAC2*
mTORC1 signaling	0.0257	2/200	*ITGB2; CXCR4*

Results are limited to OvCa-related terms.

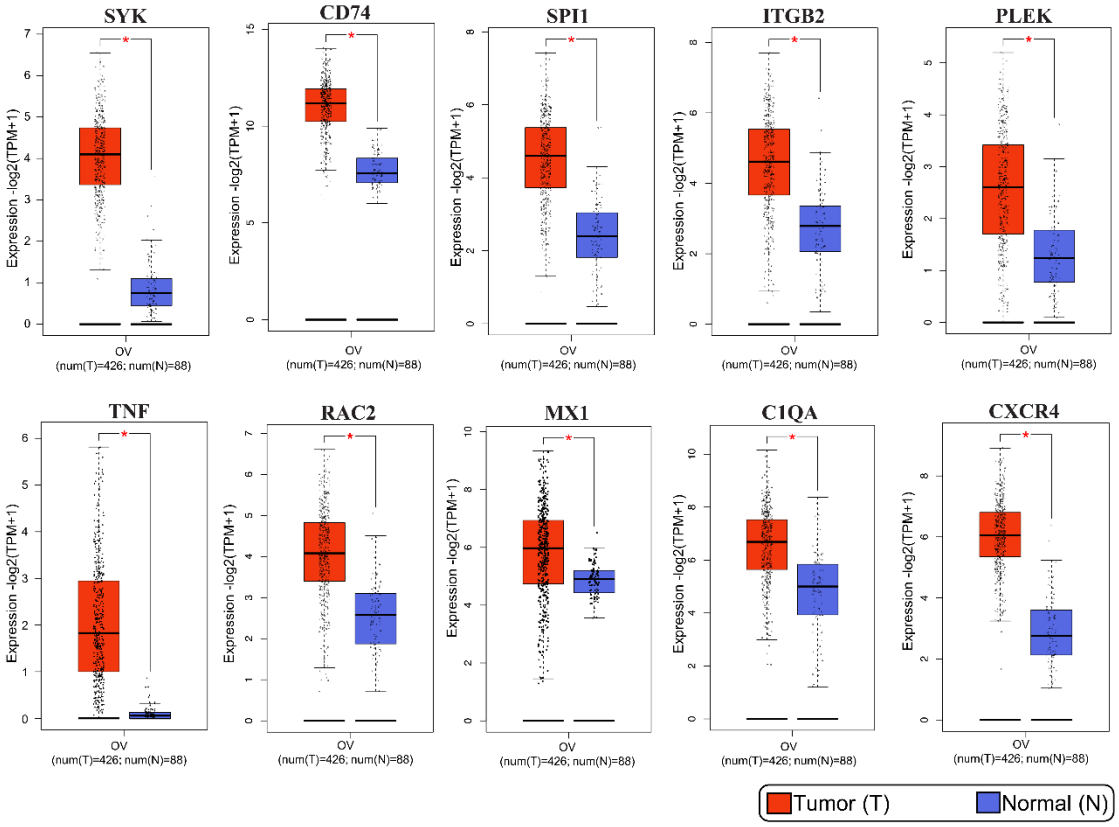

Figure 4. Overexpression of TCGA-supported DpOCSC-related hub genes in ovarian tumors. Boxplots depict $\log_2$(TPM+1) mRNA expression of SYK, CD74, SPI1, ITGB2, PLEK, TNF, RAC2, MX1, C1QA, and CXCR4 in TCGA-OV tumors (T, n=426) versus normal ovarian tissue (N, n=88). Red boxes indicate tumors and blue boxes normal samples. Asterisks denote FDR-adjusted p<0.05 (limma).

regulatory roles remain to be experimentally supported.

Assessment of hub genes at mRNA and protein levels

To assess the relevance of the identified hub genes, we examined their expression at both the mRNA and protein levels in OvCa tumors and normal ovarian tissue using TCGA and UALCAN. In TCGA-OV, the median log2(TPM+1) expression of each supported hub gene was at least 1 unit higher in tumors than in normal tissue (FDR <0.01 for all comparisons; Figure 4). Analysis of TCGA datasets showed that 10 of the 17 hub genes, namely *SYK*, *CD74*, *SPI1*, *ITGB2*, *PLEK*, *TNF*, *RAC2*, *MX1*, *C1QA*, and *CXCR4*, were expressed at substantially higher levels in OvCa tumors than in normal tissues (Figure 4).

To further investigate protein-level expression of these TCGA-supported hub genes, we used UALCAN to analyze CPTAC proteomics data. A significant elevation in the protein expression of SYK, CD74, and MX1 was observed in ovarian tumors compared to normal tissues (Figure 5A), whereas CXCR4 showed a nonsignificant trend toward higher protein levels (p= 0.74; Figure 5A). The remaining supported hub genes, *ITGB2*, *PLEK*, *RAC2*, and *C1QA*, showed lower protein expression in ovarian cancer tumors (Figure 5B). The discordance between mRNA and protein levels for several genes, such as *ITGB2*, *PLEK*, *RAC2*, and *C1QA*, may reflect post-transcriptional regulation or the contribution of immune and stromal cells in bulk tumor lysates, and therefore highlights the need for single-cell or sorted-cell evaluation. Protein expression data for TNF and SPI1 were not available in the UALCAN ovarian cancer dataset.

Functionally, SYK is a non-receptor tyrosine kinase involved in key processes regulating both immune and non-immune cells [15]. CD74, also known as the invariant chain, is overexpressed in multiple cancers and promotes tumor cell survival by activating macrophage migration inhibitory factor-dependent signaling pathways such as NF-κB and PI3K/Akt [16]. CD74 also modulates the tumor immune microenvironment, facilitating immune evasion and tumor progression, and is being explored as a therapeutic target in hematologic and solid tumors [16,17]. MX1 is an interferon-induced dynamin-like GTPase with high GTP hydrolysis activity; elevated MX1 expression has been reported in various malignancies and is functionally linked to oncogenic processes [18]. Beyond ovarian cancer, SYK and CD74 are up-regulated in 12 and 15 other cancers, respectively, and MX1 is increased in 10 distinct cancer types (Figures S3 A-C). Collectively, these mRNA, protein, and pan-cancer data support SYK, CD74, and MX1 as candidate components of immune-inflam-

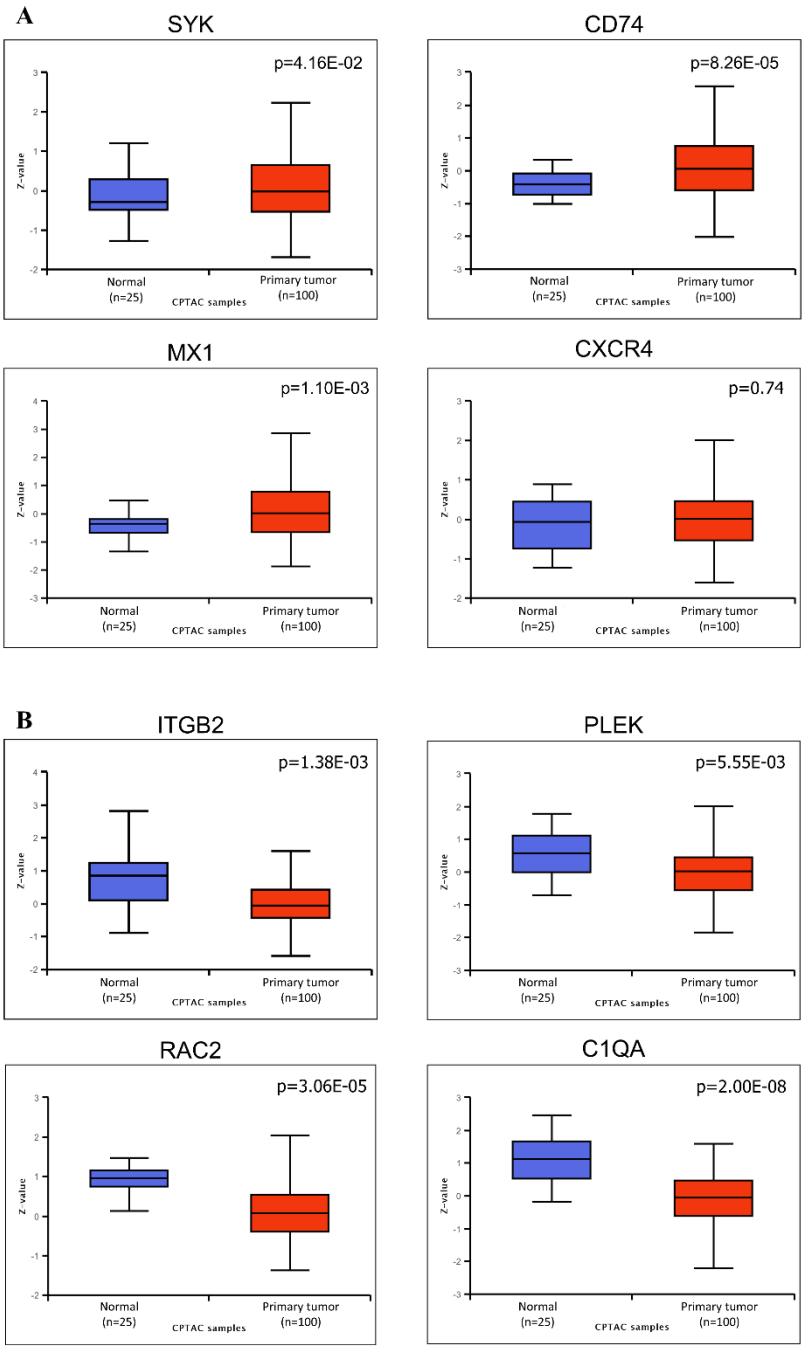

Figure 5. Protein expression of TCGA-supported hub genes in ovarian cancer. (A) UALCAN analysis of CPTAC proteomics data showing increased Z-score–normalized protein levels of SYK, CD74, MX1, and CXCR4 (non-significant) in ovarian tumors (n=100) compared with normal ovarian tissue (n=25). (B) Decreased protein levels of ITGB2, PLEK, RAC2, and C1QA in tumors versus normal tissue. p values are based on UALCAN's built-in statistical tests and are indicated in each panel.

matory programs in OvCa that merit further functional investigation.

Genetic alterations and clinical relevance of TCGA-supported hub genes

The authors next investigated genetic alterations affecting 10 of the 17 hub genes, including *SYK*, *CD74*, *SPI1*, *ITGB2*, *PLEK*, *TNF*, *RAC2*, *MX1*, *C1QA*, and *CXCR4*, all of which showed higher expression in ovarian cancer tumors than in normal tissue, using cBioPortal. Across five serous ovarian cystadenocarcinoma cohorts, these genes exhibited copy-number alterations in approximately 15-25% of tumors (Figures 6A and 6B). Deep deletions were less frequent (Figure 6A) but more common among non-supported hub genes (Figure S4).

To further clarify the importance of these hub genes in OvCa progression, their expression across disease stages using TCGA OvCa tumor data was evaluated.

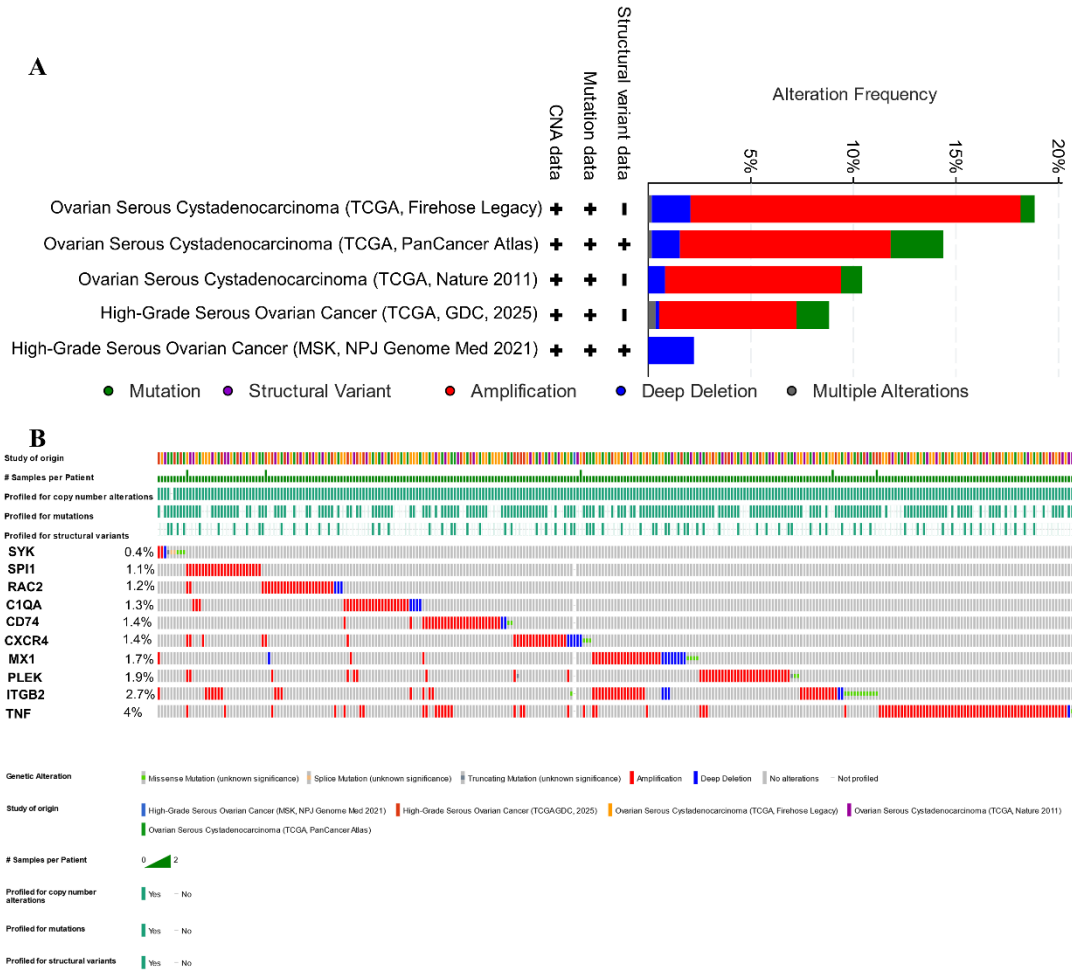

Figure 6. Somatic alterations of TCGA-supported hub genes in serous ovarian cancer. (A) Barplot summarizing overall alteration frequencies (amplification, deep deletion, mutation, multiple alterations) for 10 hub genes across five TCGA/MSK cohorts. (B) Oncoprint of gene-level copy-number and mutation events, with each column representing a tumor sample and colors indicating alteration type. Genes are ordered by total alteration frequency.

This analysis showed that TNF was significantly associated with OvCa stage (Figure 7A). In addition, the non-supported hub genes *ITGAM* and *NFKBIA* were significantly associated with distinct stages of OvCa (Figure S5A). These stage associations were statistically significant at $p<0.05$, but were not adjusted for multiple testing and should therefore be interpreted as exploratory.

MicroRNA regulation of DpOCSC-related hub genes

miRNA-target interactions were compiled from the Enrichr-linked miRTarBase resource and include both predicted and experimentally supported pairs. Also miRNA interactions with the TCGA-supported hub genes were explored. Figure 7B shows an interaction network of the top five miRNAs regulating these genes. Among the identified regulators, hsa-miR-203a-3p and hsa-miR-187-3p were linked to *TNF*, which was associated with OvCa stage. Additionally, hsa-miR-1468-5p and hsa-miR-203a-3p were linked to *SYK*. Notably, hsa-miR-146a-5p appeared to be an important epigenetic regulator of both supported and non-supported hub genes, including *ITGB2*, *CXCR4*, *NFKB1*, *TLR4*, and *RHOA* (Figure 7B and Figure S5B). Importantly, recent studies have reported over-expression of hsa-miR-146a-5p in primary OvCa tumors and omental metastases [19].

Correlation of DpOCSC-related hub genes with immune checkpoint proteins and immune-suppressive infiltrating cells

Since DpOCSCs express the pan-hematopoietic marker CD45 [10,11], we assessed the relationships between DpOCSC-related hub genes and immune checkpoint proteins to clarify their roles in ovarian cancer immunology. Pearson correlation analysis was performed between the 17 identified hub genes and six immune checkpoint proteins, including PD-L1 (CD-274), PD-1 (PDCD1), CTLA-4 (CTLA4), TIGIT, LAG-3 (LAG3), and TIM-3 (HAVCR2), in GDC-TCGA OvCa tumors [20]. The GDC-TCGA-OV cohort showed predominantly positive associations among immune-related genes. The strongest correlations were observed between *HAVCR2* and several myeloid/

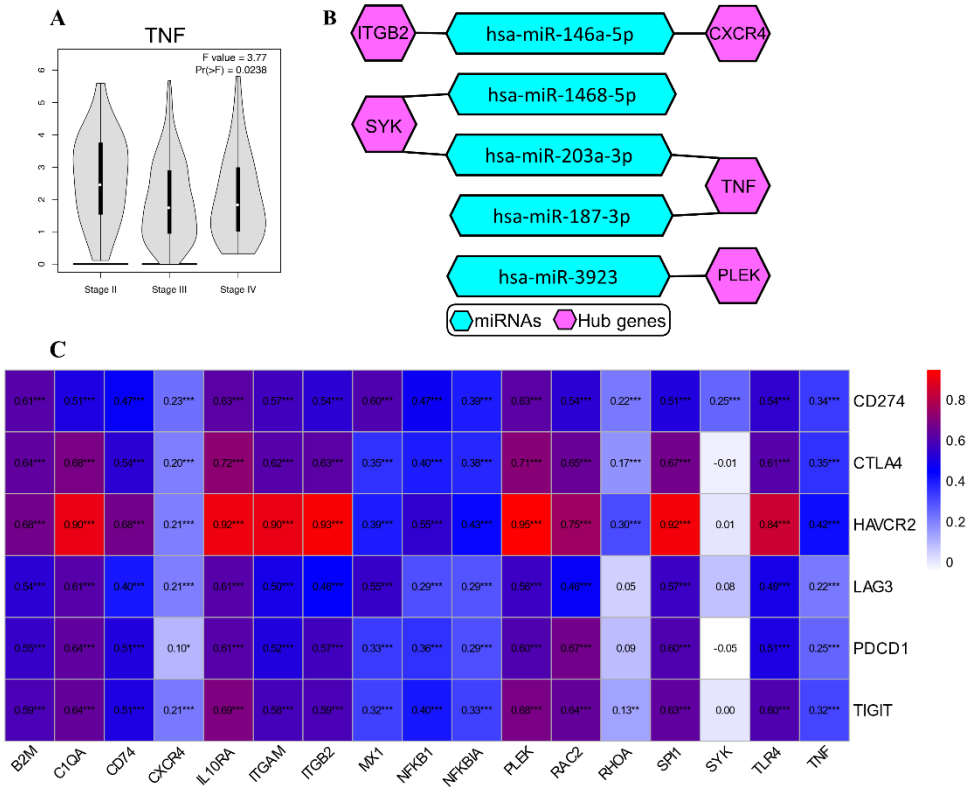

Figure 7. Clinical and regulatory features of DpOCSC-related hub genes. (A) Violin plot of TNF expression across FIGO stages II–IV in TCGA-OV. (B) Network of selected miRNAs predicted or reported to regulate TNF, SYK, ITGB2, CXCR4, and PLEK; hexagons, hub genes; cyan nodes, miRNAs. (c) Pearson correlation coefficients were calculated using $\log_2$(TPM+1)-transformed RNA-seq expression data obtained from UCSC Xena. Color intensity represents the strength and direction of the correlation (blue, weaker; red, stronger positive correlation). The numerical values within each cell indicate Pearson's correlation coefficient (r), and asterisks denote statistical significance after Benjamini–Hochberg False Discovery Rate (FDR) correction (p-value adjusted for multiple testing; adjusted p-value <0.05*, <0.01**, <0.001***).

immune markers, including *IL10RA*, *ITGAM*, *ITGB2*, *PLEK*, and *SPI1* (Pearson's r up to 0.95). Most gene pairs remained statistically significant after Benjamini-Hochberg FDR correction, whereas *CXCR4*, *RHOA*, and particularly *SYK* exhibited relatively weak correlations with several immune checkpoint genes (Figure 7C).

Various immunosuppressive cell types, including regulatory T cells (Tregs), myeloid-derived suppressor cells (MDSCs), pro-tumoral macrophages (M2 macrophages), and Cancer-Associated Fibroblasts (CAFs), are known to contribute to tumor immune escape and progression [21]. Using TIMER2.0, the correlation between infiltration levels of immune-suppressive cells and the expression of *SYK*, *CD74*, and *MX1*, which were prioritized in the present analysis was evaluated. Correlation coefficients for Tregs and M2 macrophages typically ranged from r ≈ 0.2-0.4 across algorithms, whereas negative correlations with CAFs and MDSCs were of similar magnitude but opposite direction (Figure 8 and Figure S6). These results indicate widespread positive correlations between DpOCSC-related hub genes and multiple immune checkpoint molecules, consistent with an immunosuppressive expression context but not establishing causality.

Survival analysis and prognostic value of hub genes in OvCa

To evaluate the prognostic significance of Dp-OCSC-related hub genes, univariate survival analysis for OS and Progression-Free Survival (PFS) using KM Plotter for ovarian cancer. The present analysis included data from all available datasets limited to the serous type, TCGA, and four additional datasets focused on advanced ovarian cancer, as described in table 3. Only those hub genes that showed consistent results across these datasets are report here.

The analysis of OS revealed that *SYK* and *CD74* may contribute to improved OS, whereas *MX1* was linked poorer OS (Table 3). In contrast, all three genes, *SYK*, *CD74*, and *MX1*, were associated with reduced progression-free survival in both serous ovarian carcinoma and advanced ovarian cancer. For chemo-resistant high-grade serous ovarian cancer patients, *SYK* and *MX1* were associated with better PFS outcomes (Table 3). These context-dependent associations between *SYK*, *CD74*, and *MX1* and OS or PFS may reflect differences in cohort composition, treatment history, or the limitations of univariate survival analyses, and should therefore be considered exploratory. All survival analyses were performed using univariate

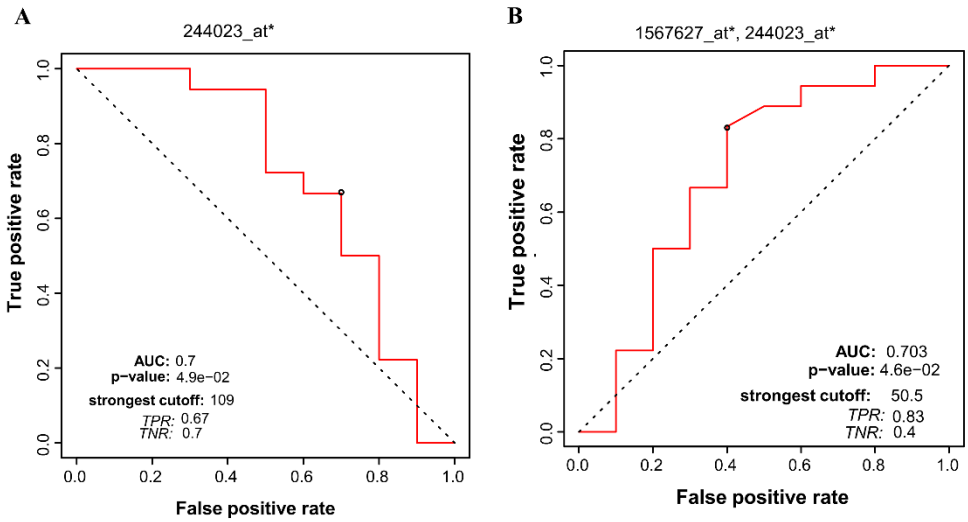

Figure 8. Association of SYK, CD74, and MX1 with immune-suppressive cell infiltration. Scatter plots show correlations between (A) *SYK*, (B) *CD74* and (C) *MX1* gene expression (log_2TPM) and estimated levels of tumor purity, Tregs, CAFs, MDSCs, and macrophage M2 across TCGA-OV tumors using representative algorithms (*e.g.*, QUANTISEQ, XCELL, TIDE). Blue lines indicate fitted regression; r and p values are reported in each panel.

Table 3 Association of mRNA- and protein-evaluated hub genes with overall survival and progression-free survival

Hub genes	HR	Logrank p	Dataset	Samples
Overall Survival (OS)				
CD74	0.82 (0.71-0.96)	0.012	All	Serous ovarian carcinoma (n=1207)
SYK	0.59 (0.41-0.86)	0.0053	GSE9891	Frozen tissue of ovary, Fallopian tube, or peritoneum carcinoma (n=285)
CD74	0.66 (0.45-0.96)	0.028		
CD74	0.41 (0.22-0.77)	0.0041	GSE18520	Advanced stage ovarian carcinoma (n=53)
MX1	2 (1.02-3.92)	0.04	GSE30161	Treated OvCa patients with III-IV stages (n=54)
MX1	1.58 (1-2.5)	0.049	GSE26193	High-grade ovarian carcinoma (n=107)
Progression-Free Survival (PFS)				
SYK	1.32 (1.12-1.56)	0.00084	All	Serous ovarian carcinoma (n=1104)
MX1	1.2 (1.04-1.4)	0.014		
MX1	1.58 (1.01-2.46)	0.043	GSE26193	High-grade ovarian carcinoma (n=107)
SYK	0.7 (0.52-0.93)	0.013	GSE9891	Frozen tissue of ovary, Fallopian tube, or peritoneum carcinoma (n=285)
MX1	1.86 (1.33-2.61)	0.00026		
SYK	0.53 (0.3-0.93)	0.026	GSE30161	Treated OvCa patients with III-IV stages (n=54)
CD74	1.99 (1.11-3.58)	0.02		
MX1	1.98 (1.1-3.56)	0.021		
SYK	0.09 (0.02-0.33)	6.50E-06	GSE51373	Including 12 chemoresistant and 16 sensitive chemotherapy HGSOCs (n=28)
MX1	0.28 (0.1-0.74)	0.007		

HGSOC: High-Grade Ovarian Serous Carcinoma.

log-rank tests in KM Plotter; therefore, these associations should be regarded as hypothesis-generating and require evaluation in multivariable models.

SYK as a biomarker reveals higher diagnostic value in OvCa

SYK, CD74, and MX1 were evaluated as biomarkers for 6-month recurrence-free survival. SYK alone approached significant diagnostic performance in any- and platinum-based chemotherapy, with AUC >0.7 under paclitaxel (PTX) (Figure 9A). Multi-gene combinations (SYK+CD74, SYK+MX1, SYK+CD74+MX1) did not outperform SYK alone in any- or platinum-based chemotherapy. Under PTX, the SYK–CD74 combination improved diagnostic performance

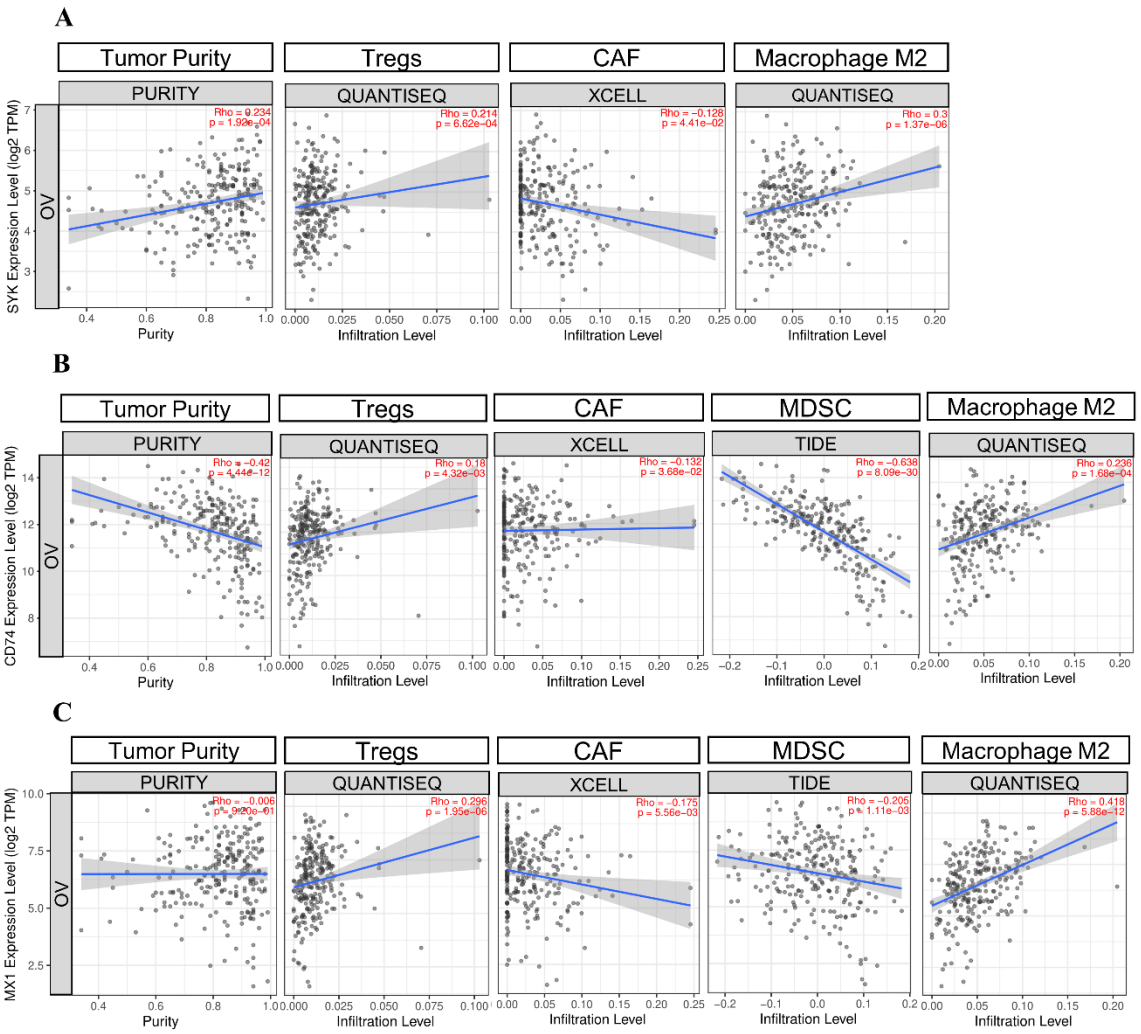

Figure 9. Diagnostic performance of SYK and its combinations as predictors of 6-month relapse. ROC curves from ROC Plotter for (A) SYK alone and (B) and its combination with CD74 under paclitaxel, respectively. AUC, P value, and optimal cut-off with corresponding True-Positive Rate (TPR) and True-Negative Rate (TNR) are shown in each panel.

(Figure 9B), suggesting utility for predicting 6-month relapse in this context.

Clinico-pathological evaluation of hub genes

To assess the clinical relevance of DpOCSC-related hub genes, we examined their associations with selected clinicopathological variables in TCGA ovarian cancer data using chi-square tests of independence. *SPI1*, *ITGB2*, *PLEK*, *C1QA*, and *CXCR4* were significantly associated with lymphatic invasion, whereas *ITGB2*, *PLEK*, *C1QA*, and *CXCR4* were also associated with venous invasion (Table 4). *SYK* was associated with new neoplasm event type, and *SYK*, *TNF*, and *MX1* were associated with primary therapy outcome success. Because these analyses were based on dichotomized expression values and univariate categorical comparisons, the findings should be considered exploratory. Association for non-supported DpOCSC-related hub genes with these features are presented in Table S6.

Table 4. Association of TCGA-supported hub genes with clinico-pathological features

Clinical significance	Hub genes
Lymphatic invasion [a]	*SPI1* **, *ITGB2* ***, *PLEK* ****, *C1QA* ***, *CXCR4* *
Venous invasion [a]	*ITGB2* **, *PLEK* ****, *C1QA* **, *CXCR4**
New neoplasm event type [b]	*SYK* *
Primary therapy outcome success [c]	*SYK* *, *TNF* *, *MX1* **

a: Yes/No, b: Metastatic/Locoregional disease/Progression of disease/ Recurrence, c: Partial remission/Stable disease/ Progressive disease/Complete remission (* p<0.05, ** p<0.01, *** p<0.001, **** p<0.0001).

Given the clinical challenges posed by ovarian cancer, especially recurrence and chemoresistance, these associations may be relevant to disease progression and treatment response. However, because these analyses were based on dichotomized expression values and univariate comparisons, they should be interpreted as

Table 5. Predicted modulation of TCGA-supported hub genes by signaling pathways in OCSCs

Signaling pathways	Evidence source/ Platform	Hub genes
Wnt/β-catenin-TCF/LEF	TRANSFAC and JASPAR	*SYK* (LEF1); *CD74* (TCF, LEF1); *ITGB2* (LEF1); *PLEK* (LEF1); *TNF* (TAL1::TCF3); *RAC2* (TCF3); *MX1* (TCF3, LEF1); *C1QA* (TCF4)
	JASPAR PWM human 2025	*SYK* (TCF3); *CD74* (TCF4); *SPI1* (TCF3); *PLEK* (TAL1::TCF3); *RAC2* (TCF3); *MX1* (TCF4)
STAT3	JASPAR PWM human 2025	*ITGB2* (STAT3)
TGFβ/Smad2/3/4	ChEA 2022 and ChIP-seq 2015	*RAC2* (SMAD4 in A2780)
	TRANSFAC and JASPAR	*MX1* (SMAD4)
	JASPAR PWM human 2025	*ITGB2* (SMAD2); *CXCR4* (SMAD2)
NFκB	TRUST 2019	*CD74* (NFKB1)*; TNF* (NFKB1)*; CXCR4* (NFKB1)
	TRANSFAC and JASPAR	TNF (NFKB1); *C1QA* (NFKB1)*; CXCR4* (NFKB1)
	JASPAR PWM human 2025	*CD74* (NFKB2); *TNF* (NFKB1, NFKB2); *C1QA* (NFKB1)*; CXCR4* (NFKB1)
Notch	TRANSFAC and JASPAR	*SYK* (RBPJ); *CD74* (RBPJ)
	JASPAR PWM human 2025	*SYK* (RBPJ); *CXCR4* (RBPJ)
Hippo-YAP1-TEAD	TRANSFAC and JASPAR	*ITGB2* (TEAD2); *TNF* (TEAD1); *C1QA* (TEAD2); *CXCR4* (TEAD4)
	JASPAR PWM human 2025	*SYK* (TEAD1, TEAD3); *RAC2* (TEAD4); *C1QA* (TEAD1); *CXCR4* (TEAD3, TEAD4)

Note: Predictions were generated using motif- and database-based resources, and one ChIP-seq-supported interaction was identified in A2780 ovarian cancer cells. A2780 is an ovarian cancer cell line derived from an untreated patient. These results are predictive and require experimental evaluation in DpOCSCs.

exploratory and hypothesis-generating rather than as evidence of causality.

Predicted upstream regulatory context of DpOCSC-related hub genes

To explore potential upstream regulatory contexts, we analyzed predicted transcription factor binding for the TCGA-supported hub genes using six signaling pathways relevant to ovarian cancer stem cells: STAT3, TGFβ/Smad2/3/4, Hippo-YAP1/TAZ-TEAD, NF-κB, Notch/RBPJ, and Wnt/β-catenin-TCF/LEF (13). TF–target relationships were compiled from ChEA 2022, ENCODE TF ChIP-seq 2015, TRUST 2019, TRANSFAC, and JASPAR PWM databases (Table 5; Supplementary Table S7). Among the inferred regulators, Wnt/β-catenin signaling was the most frequently predicted, with LEF1, TCF3, TCF4, and TAL1: TCF3 motifs detected in the promoters of SYK, CD74, ITGB2, PLEK, TNF, RAC2, MX1, and C1QA across TRANSFAC, JASPAR, and JASPAR PWM human 2025. NF-κB was also strongly implicated, with NFKB1/NFKB2 sites predicted for CD74, TNF, C1QA, and CXCR4 in TRUST 2019 and TRANSFAC/JASPAR. Hippo/YAP1-TEAD components (TEAD1-4) showed predicted interactions with SYK, ITGB2, TNF, RAC2, C1QA, and CXCR4, whereas Notch (RBPJ) and STAT3 appeared less frequently, targeting SYK, CD74, CXCR4, and ITGB2. TGFβ/Smad2/3/4 predictions were sparse, limited to RAC2 (SMAD4 *via* ChEA 2022 in A2780 cells), MX1 (SMAD4 *via* TRANSFAC/JASPAR), and ITGB2/CXCR4 (SMAD2 *via* JASPAR PWM). These predictions should be interpreted cautiously, because several source ChIP-seq datasets derive from non-ovarian and non-CSC cell lines, and the motifs themselves are database-based inferences rather than direct experimental evidence in DpOCSCs. Thus, while these analyses suggest possible involvement of Wnt/β-catenin, NF-κB, Hippo, and, to a lesser extent, TGFβ and Notch pathways, they remain hypothesis-generating. Experimental follow-up, such as ChIP-qPCR, reporter assays, or CRISPR-based perturbation in DpOCSC or relevant ovarian cancer models, will be required to confirm direct transcriptional regulation.

Discussion

OCSCs are a biologically important subpopulation within ovarian tumors and have been implicated in tumor initiation, metastasis, chemoresistance, and recurrence [22,23]. In this context, stem-like EpCAM/ CD45 dual-positive ovarian cancer cells isolated from malignant ascites may represent a rare and aggressive subpopulation associated with recurrent disease, although their biological origin and emergence remain incompletely defined [11]. Recent pilot data further suggested that circulating $EpCAM^+/CD45^+$ extracellular vesicles were associated with platinum response in high-grade serous ovarian cancer [24]. This recent study may suggest that post-chemotherapy increases in $EpCAM^+CD45^+$ EVs may not only relate to tumor cell death and debris release but could also be influenced by therapy-associated enrichment of resistant $EpCAM^+CD45^+$ tumor subsets and by immune-tumor interactions that generate EVs carrying both epithelial and leukocyte markers [24]. Ascites may further shape this biology by providing a permissive and immunologically active microenvironment that supports tumor adaptation and stemness-associated programs [25,26].

The present transcriptomic analysis suggests that this DpOCSC population is enriched for inflammatory and immune-related signaling. The prioritized hub

genes were linked to interferon- and TNF/NF-κB-associated pathways, and several genes showed positive associations with immune-cell subsets and immune-related markers, consistent with the highly immunomodulatory nature of the ovarian cancer ascites microenvironment [25]. Rather than implying a specific mechanism, these findings support a model in which DpOCSCs occupy an immune-inflamed and therapy-resistant state.

Among the prioritized hub genes, *SYK*, *CD74*, and *MX1* were particularly notable because they integrated inflammatory signaling, immune regulation, and clinical associations in OvCa. *SYK* is a non-receptor tyrosine kinase involved in immune signaling and is being explored as a therapeutic target in malignancies [15]. In this analysis, *SYK* was overexpressed and frequently amplified in ovarian tumors, was associated with immune-related marker expression and immune-cell infiltration and showed exploratory associations with overall and progression-free survival, as well as AUC values around 0.7 for short-term relapse prediction. These results are compatible with emerging evidence that SYK contributes to chemoresistance and may regulate stem-like properties in ovarian cancer, but our data remains correlative and hypothesis-generating [27-29]. Recent work also showed that SYK overexpression promotes resistance to DNA-targeted therapy in high-grade serous ovarian cancer, further supporting its relevance to aggressive disease biology [30]. CD74, the invariant chain and receptor component for MIF signaling, is overexpressed in ovarian cancer and has been linked to poor clinical outcome and invasion [16,17,31]. CD74 can engage PI3K/Akt and ERK/MAPK pathways and may promote survival programs relevant to chemoresistance, EMT, and spheroid maintenance [32,33]. MX1, an interferon-induced GTPase, was similarly overexpressed, enriched in interferon-response modules, and has been associated with poor outcome or treatment resistance in prior cancer studies [18,34]. Spatial profiling data from ovarian cancer further supports an interferon-rich and immune-suppressive microenvironment, with MX1 appearing within that broader interferon-stimulated context [35]. Together, these findings support a model in which SYK, CD74, and MX1 participate in an inflammatory, immune-modulated transcriptional state associated with DpOCSC biology.

The observed copy-number patterns are consistent with an association between genomic alteration and aggressive biology. Prioritized DpOCSC-related hub genes were more amplified, whereas genes outside this core set more frequently harbored deep deletions, a pattern consistent with prior reports linking copy-number changes to chemoresistance in ovarian cancer [36,37]. Although our cross-sectional cBioPortal analysis cannot establish causality, it is consistent with the idea that inflammatory signaling, genomic instability, and aggressive disease biology may co-occur in DpOCSC-enriched tumors.

The prioritized hub genes also showed associations with invasion-related features. Enhanced migratory and invasive behavior is a recognized property of aggressive OCSC populations, and in this analysis several hub genes correlated with lymphatic and venous. This observation is consistent with prior evidence that $EpCAM^+/CD45^+$-positive ovarian cancer cells can exhibit invasive and stem-like traits [11].

Conclusion

Taken together, the literature and the present *in silico* results point to SYK-associated inflammatory signaling as a candidate pathway for further investigation in DpOCSCs. However, the current study does not establish direct functional roles for *SYK*, *CD74*, or *MX1* in stemness, and their elevated expression may reflect an aggressive immune-inflamed state rather than a direct contributing mechanism. Functional studies in DpOCSCs will be required to determine whether these genes regulate stem-like behavior, invasion, or therapy resistance.

This study has limitations that should be considered when interpreting the findings. The DpOCSC group was small, and the analyses were therefore exploratory. In addition, the use of public datasets from different platforms and cohorts may introduce residual heterogeneity despite normalization and batch correction. The observed survival, immune, and clinicopathological associations are therefore best regarded as supportive signals that warrant evaluation in larger cohorts. Moreover, the $EpCAM^+/CD45^+$ phenotype identifies a distinct ascites-derived cell population, but its precise biological origin and functional significance remain to be clarified. Future experimental work will be essential to define the mechanistic roles of *SYK*, *CD74*, *MX1*, and related hub genes in DpOCSC biology.

In summary, comparative transcriptomic analysis of stem-like DpOCSCs versus other ascites-derived OCSC populations identified an interferon- and TNF-dominated inflammatory module containing 17 up-regulated hub genes. Among these, *SYK*, *CD74*, and *MX1* were consistently overexpressed in our analyses and may contribute to frequent copy-number gain, immune-related features, and exploratory clinical outcome metrics in large OvCa cohorts (Figure 10). These findings nominate SYK-associated inflammatory signaling as a candidate axis for mechanistic and translational studies in recurrent, ascites-rich ovarian cancer.

Data availability statement

The datasets analyzed during the current study are available in the National Center for Biotechnology Information (NCBI)- Gene Expression Omnibus (GEO) database (https:/www.ncbi.nlm.nih.gov/geo/) with ac-

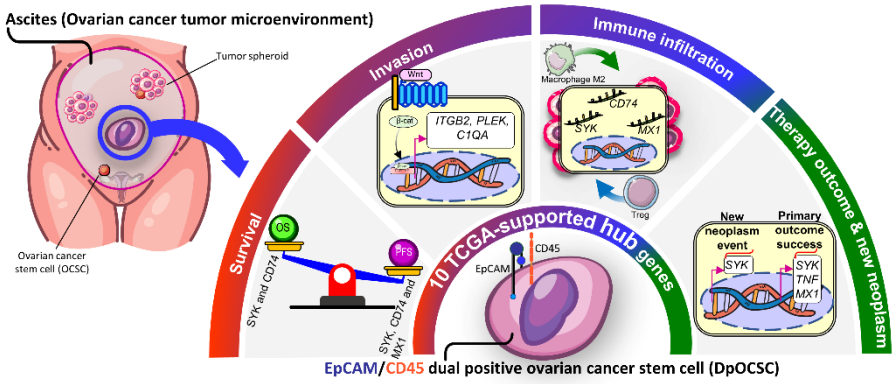

Figure 10. Comparative transcriptome profiling of ascites derived EpCAM/CD45 dual-positive ovarian cancer stem cells versus other ascites derived OCSC population identified 10 TCGA-supported hub genes. Three of them were additionally confirmed at the protein level and were associated with survival, immune infiltration, new neoplasm event and outcome success. Wnt signaling emerged as a major regulator of these genes, particularly in the context of tumor invasion.

cession numbers GSE75036, GSE90125 and GSE-216627, Enrichr database (https://amp.pharm.mssm.edu/Enrichr/), Bioconductor package (v3.17) for R (version 4.3.1) (https://www.r-ptoject.org), GraphPad Prism9 software (https://www.graphpad. com), SRplot online tool (https://www.bioinformatics. com.cn/en), Volcano plot online tool (https://huygens. science.uva.nl/VolcaNoseR2/), String (v1.7.1), CentiScape (v2.1) and Cytohubba (v0.1) plugins for Cytoscape software (v3.10.0) (https://cytoscape.org/), GEPIA database (http://gepia.cancer-pku.cn), UALCAN database (https://ualcan.path.uab.edu/), cBioPortal database (http://cbioportal.org), KM plotter database (https://kmplot.com), ROC Plotter database (https://rocplot.org), UCSC Xena Browser database (http://xenabrowser.net), Cut-off Finder online tool (https://molpathoheidelberg.shinyapps.io/CutoffFinder_v1/), Timer 2.0 database (http://timer.cistrome.org/) and the R code generated for clinco-pathological analysis on Github (https://github.com/sadra-daneshvari/OvarianCancerProject). All data generated and analyzed in this study can be found in these databases.

Conflict of Interest

The authors declare no competing interests.

Funding: This work was supported by grant #268308/k6/034 by university of Tehran.

References

1. Jayson GC, Kohn EC, Kitchener HC, Ledermann JA. Ovarian cancer. Lancet 2014;384(9951):1376-88.
2. Mills K, Fuh K. Recent advances in understanding, diagnosing, and treating ovarian cancer. F1000Res 2017;6:84.
3. Kindelberger DW, Lee Y, Miron A, Hirsch MS, Feltmate C, Medeiros F, et al. Intraepithelial carcinoma of the fimbria and pelvic serous carcinoma: evidence for a causal relationship. Am J Surg Pathol 2007;31(2):161-9.
4. Auersperg N. Ovarian surface epithelium as a source of ovarian cancers: unwarranted speculation or evidence-based hypothesis? Gynecol Oncol 2013;130(1):246-51.
5. Yeung T-L, Leung CS, Yip K-P, Au Yeung CL, Wong ST, Mok SC. Cellular and molecular processes in ovarian cancer metastasis. A review in the theme: cell and molecular processes in cancer metastasis. Am J Physiol Cell Physiol 2015;309(7):C444-C56.
6. Kim S, Kim B, Song YS. Ascites modulates cancer cell behavior, contributing to tumor heterogeneity in ovarian cancer. Cancer Sci 2016;107(9):1173-8.
7. Al-Alem LF, Pandya UM, Baker AT, Bellio C, Zarrella BD, Clark J, et al. Ovarian cancer stem cells: What progress have we made? Int J Biochem Cell Biol 2019;107:92-103.
8. Wilczyński JR, Wilczyński M, Paradowska E. Cancer Stem Cells in Ovarian Cancer-A Source of Tumor Success and a Challenging Target for Novel Therapies. Int J Mol Sci 2022;23(5):2496.
9. Romeo E, Caserta CA, Rumio C, Marcucci F. The vicious cross-talk between tumor cells with an EMT phenotype and cells of the immune system. Cells 2019;8(5):460.
10. Ramakrishnan M, Mathur SR, Mukhopadhyay A. Fusion-derived epithelial cancer cells express hematopoietic markers and contribute to stem cell and migratory phenotype in ovarian carcinoma. Cancer Res 2013;73(17):5360-70.
11. Akhter MZ, Sharawat SK, Kumar V, Kochat V, Equbal Z, Ramakrishnan M, et al. Aggressive serous epithelial ovarian cancer is potentially propagated by EpCAM(+)CD45(+) phenotype. Oncogene 2018;37(16):2089-103.
12. Kanehisa M, Goto S. KEGG: kyoto encyclopedia of genes and genomes. Nucleic Acids Res 2000;28(1):27-30.
13. Muñoz-Galván S, Carnero A. Targeting cancer stem cells to overcome therapy resistance in ovarian cancer. Cells 2020;9(6):1402.

14. Budczies J, Klauschen F, Sinn BV, Győrffy B, Schmitt WD, Darb-Esfahani S, et al. Cutoff Finder: a comprehensive and straightforward Web application enabling rapid biomarker cutoff optimization. PloS One 2012;7 (12):e51862.
15. Shao Y, Zhang S, Zhang Y, Liu Z. Recent advance of spleen tyrosine kinase in diseases and drugs. Int Immunopharmacol 2021;90:107168.
16. Schröder B. The multifaceted roles of the invariant chain CD74 — More than just a chaperone. Biochim Biophys Acta 2016 Jun;1863(6 Pt A):1269-81.
17. Li RQ, Yan L, Zhang L, Zhao Y, Lian J. CD74 as a prognostic and M1 macrophage infiltration marker in a comprehensive pan-cancer analysis. Sci Rep 2024;14(1): 8125.
18. Aljohani AI, Joseph C, Kurozumi S, Mohammed OJ, Miligy IM, Green AR, et al. Myxovirus resistance 1 (MX1) is an independent predictor of poor outcome in invasive breast cancer. Breast Cancer Res Treat 2020; 181:541-51.
19. Wilczyński M, Żytko E, Szymańska B, Dzieniecka M, Nowak M, Danielska J, et al. Expression of miR-146a in patients with ovarian cancer and its clinical significance. Oncol Lett 2017;14(3):3207-14.
20. Hao W, Zhao H, Li Z, Li J, Guo J, Chen Q, et al. Identification of potential markers for differentiating epithelial ovarian cancer from ovarian low malignant potential tumors through integrated bioinformatics analysis. J Ovarian Res 2021;14(1):46.
21. Tie Y, Tang F, Wei Y-q, Wei X-w. Immunosuppressive cells in cancer: mechanisms and potential therapeutic targets. J Hematol Oncol 2022;15(1):61.
22. Alvero AB, Chen R, Fu HH, Montagna M, Schwartz PE, Rutherford T, et al. Molecular phenotyping of human ovarian cancer stem cells unravels the mechanisms for repair and chemoresistance. Cell Cycle 2009;8(1):158-66.
23. Bapat SA, Mali AM, Koppikar CB, Kurrey NK. Stem and progenitor-like cells contribute to the aggressive behavior of human epithelial ovarian cancer. Cancer Res 2005;65(8):3025-9.
24. Tersigni C, Onori M, Buzzonetti A, Ferrante A, Fattorossi A, Battaglia A, et al. Diagnostic performance of circulating EpCAM+ and CD45+ extracellular vesicles in platinum-sensitivity in high-grade serous ovarian cancer: a pilot study. J Ovarian Res 2025;18(1):93.
25. Almeida-Nunes DL, Mendes-Frias A, Silvestre R, Dinis-Oliveira RJ, Ricardo S. Immune Tumor Microenvironment in Ovarian Cancer Ascites. Int J Mol Sci 2022;23 (18):10692.
26. Rickard BP, Conrad C, Sorrin AJ, Ruhi MK, Reader JC, Huang SA, et al. Malignant ascites in ovarian cancer: cellular, acellular, and biophysical determinants of molecular characteristics and therapy response. Cancers (Basel)) 2021;13(17):4318.
27. Gaillard S, Wilkinson M, Martin LP, Deery A, Langsdale A, Bayable A, et al. A phase 1 study of the SYK inhibitor fostamatinib and weekly paclitaxel for recurrent platinum-resistant ovarian cancer. American Society of Clinical Oncology 2023.
28. Mandal J, Jones TN, Liberto JM, Gaillard S, Wang T-L, Shih I-M. Dual Inhibition of SYK and EGFR Overcomes Chemoresistance by Inhibiting CDC6 and Blocking DNA Replication. Cancer Res 2024 Nov 15;84(22): 3881-3893.
29. Yu Y, Suryo Rahmanto Y, Lee MH, Wu PH, Phillip JM, Huang CH, et al. Inhibition of ovarian tumor cell invasiveness by targeting SYK in the tyrosine kinase signaling pathway. Oncogene 2018;37(28):3778-89.
30. Zhou Q, Tu X, Hou X, Yu J, Zhao F, Huang J, et al. Syk-dependent homologous recombination activation promotes cancer resistance to DNA targeted therapy. Drug Resist Updat 2024;74:101085.
31. Lee YS, Baek JM, Park EK, Kim CJ, Lee HJ, Kim JO. Expression and therapeutic potential of macrophage migration inhibitory factor and CD74 in ovarian cancer. European Journal of Gynaecological Oncology 2020;41 (1):65-9.
32. Becker-Herman S, Arie G, Medvedovsky H, Kerem A, Shachar I. CD74 Is a Member of the Regulated Intramembrane Proteolysis-processed Protein Family. Mol Biol Cell 2005;16(11):5061-9.
33. Oliveira CS, de Bock CE, Molloy TJ, Sadeqzadeh E, Geng XY, Hersey P, et al. Macrophage migration inhibitory factor engages PI3K/Akt signalling and is a prognostic factor in metastatic melanoma. BMC Cancer 2014;14(1):630.
34. Yang Y, Chen L, Xu L, Fan Z, Lu Y, Ji T, et al. Genes associated with platinum-resistance in platinum-resistant ovarian cell line. European Journal of Gynaecological Oncology 2018;39(2):257.
35. Kader T, Lin JR, Hug CB, Coy S, Chen YA, de Bruijn I, et al. Multimodal Spatial Profiling Reveals Immune Suppression and Microenvironment Remodeling in Fallopian Tube Precursors to High-Grade Serous Ovarian Carcinoma. Cancer Discov 2025;15(6):1180-202.
36. Gorski JW, Ueland FR, Kolesar JM. CCNE1 Amplification as a Predictive Biomarker of Chemotherapy Resistance in Epithelial Ovarian Cancer. Diagnostics (Basel) 2020;10(5):279.
37. Kolasa IK, Rembiszewska A, Felisiak A, Ziolkowska-Seta I, Murawska M, Moes J, et al. PIK3CA amplification associates with resistance to chemotherapy in ovarian cancer patients. Cancer Biol Ther 2009;8(1):21-6.

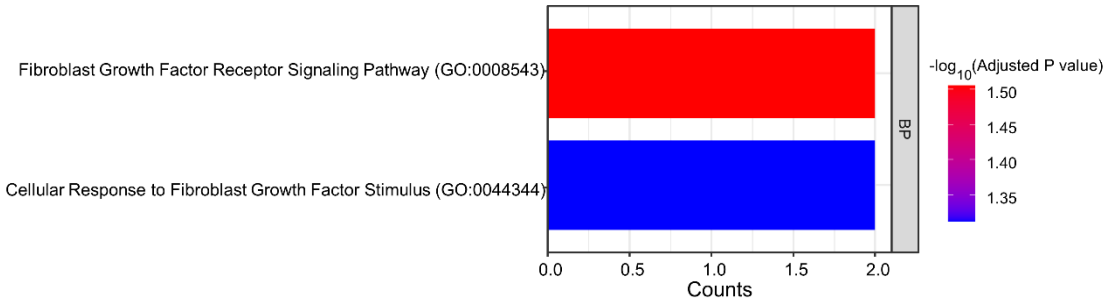

Figure S1. Enrichment analysis of down-regulated genes in DpOCSCs. Selected GO biological Process (BP) terms for down-regulated genes (adj. p-value <0.05).

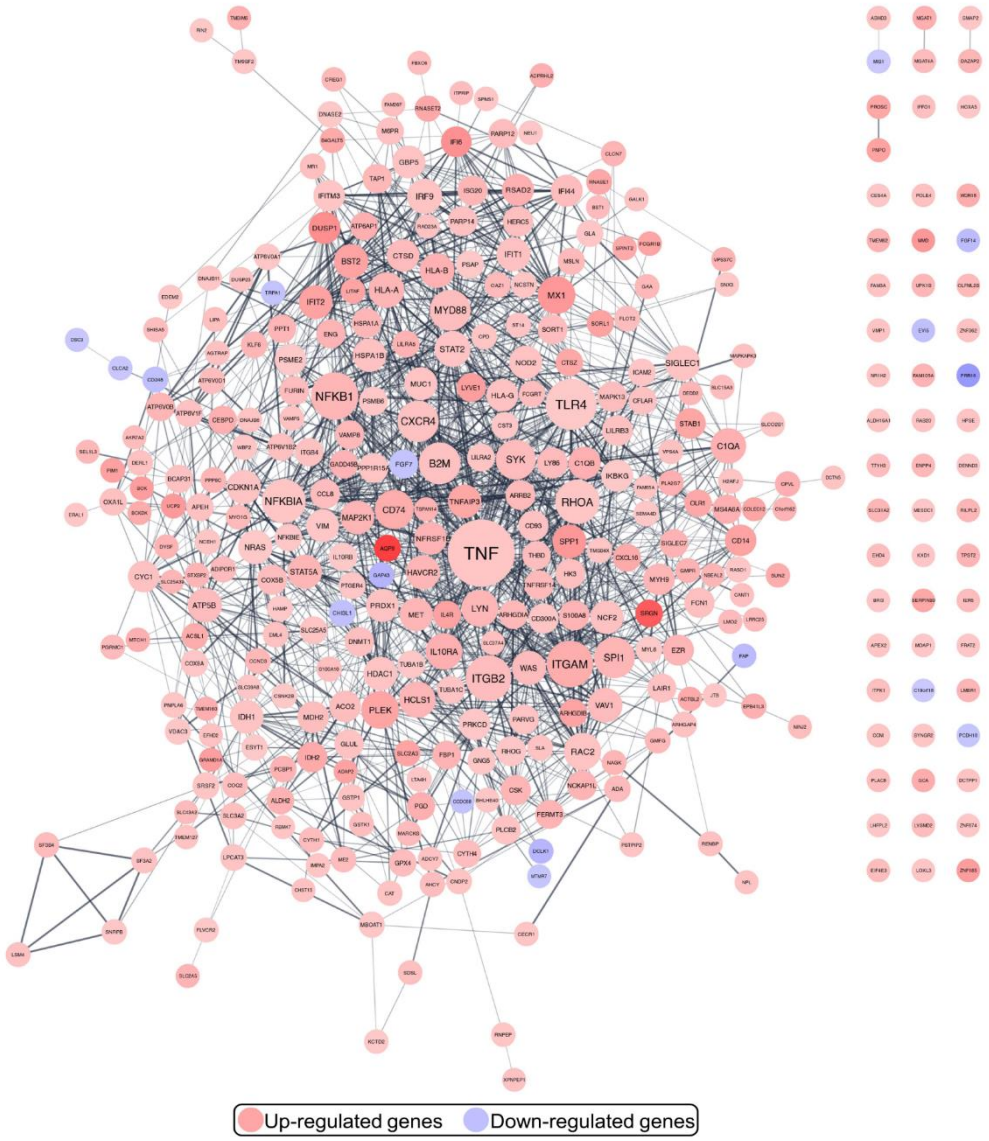

Figure S2. Construction of a protein-protein interaction (PPI) network for differentially expressed genes.Red to pink and lilac to dried lilac color spectrum nodes indicate up-regulated (Log2FC range 3.5512 - 1.0002) and down-regulated (Log2FC range -1.884- -1.093) genes, respectively, with node size representing the degree of each node thickness of edges represents confidence score of interaction (>0.4).

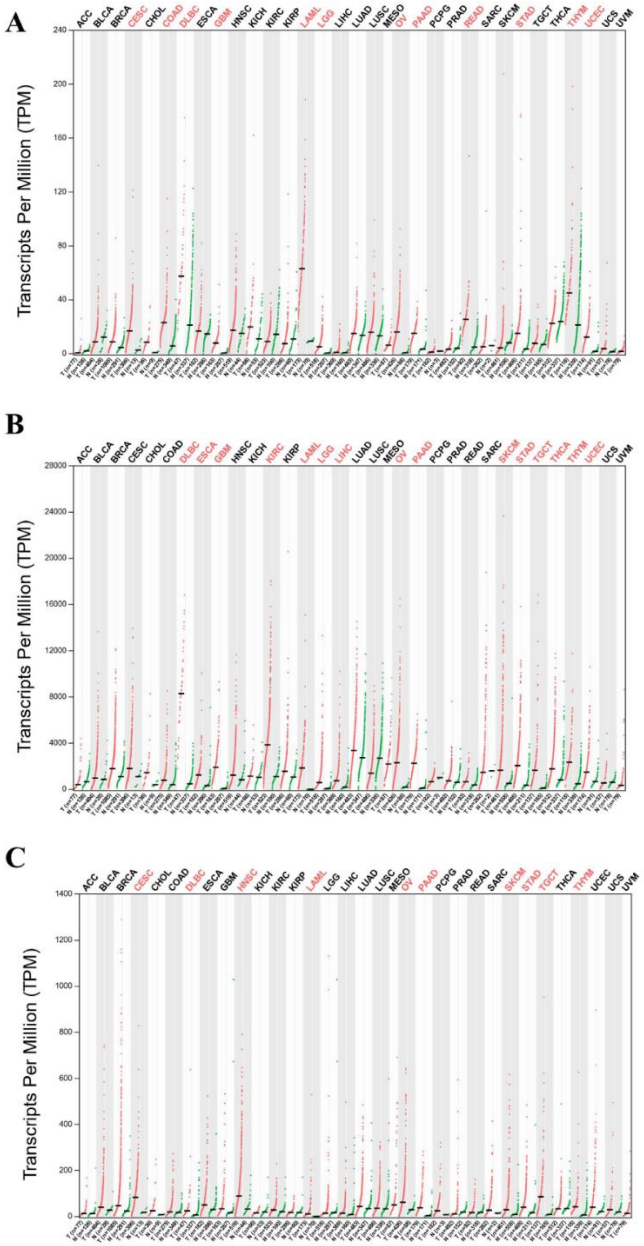

Figure S3. Expression of SYK, CD74, and MX1 across various cancers based on TCGA. (A) SYK (B) CD74 and (C) MX1. Red indicates significant up-regulation, green signifies considerable down-regulation (|Log2FC|>1 and qvalue <0.01), while black denotes non-considerable expression in various cancers.

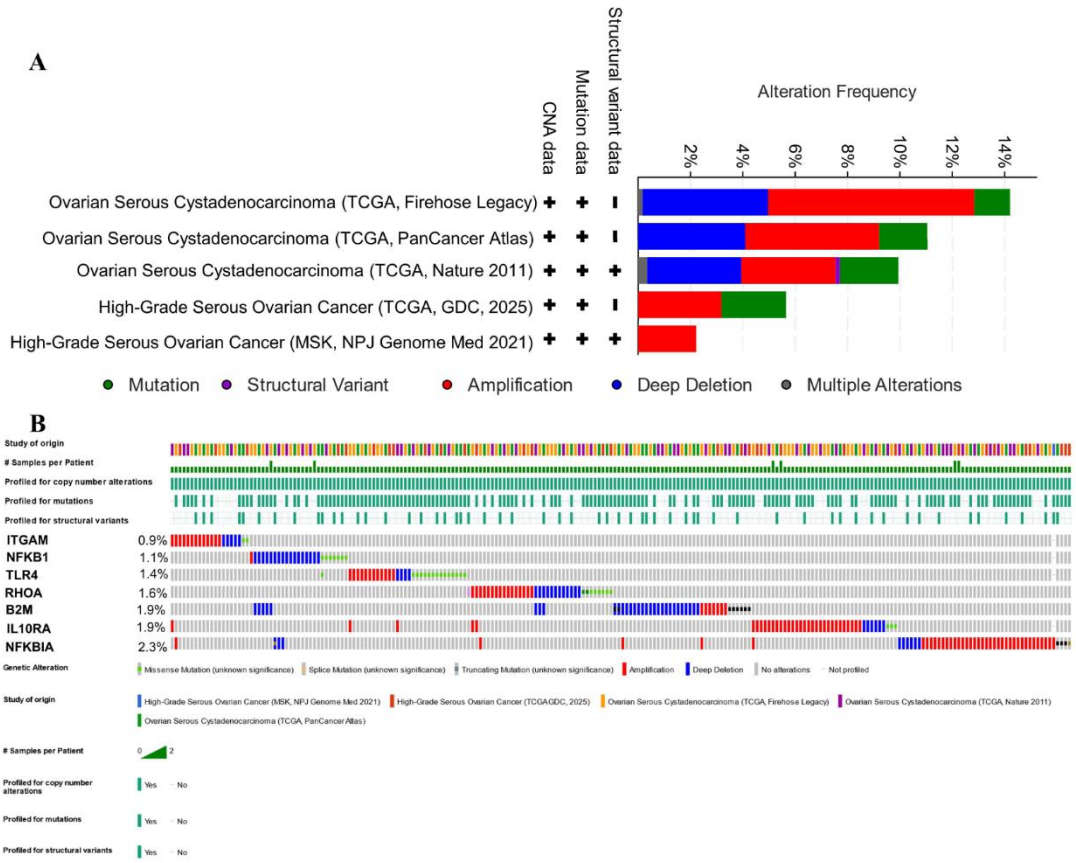

Figure S4. Genetic alterations of non-supported hub genes. (A) Summary of genetic alterations (B) OncoPrint panel illustrating genetic alterations.

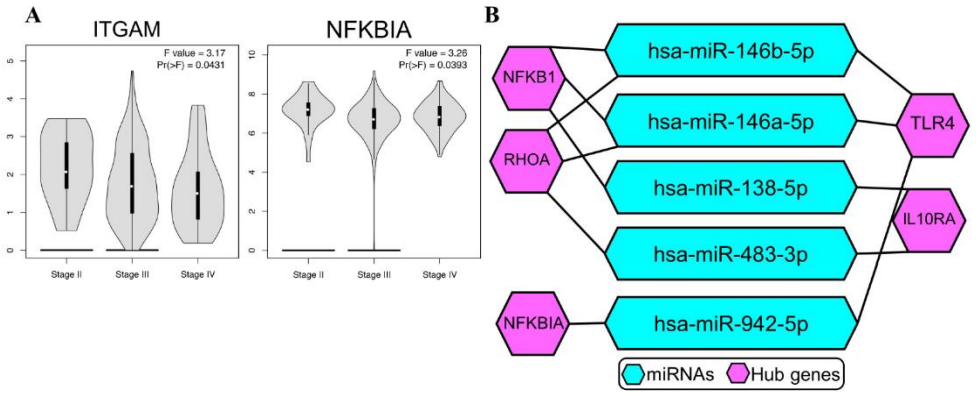

Figure S5. Stage plots and miRNA-hub gene interaction network of non-supported hub genes. (A) Stage plots (B) Top 5 miRNA-non-supported hub gene interaction network.

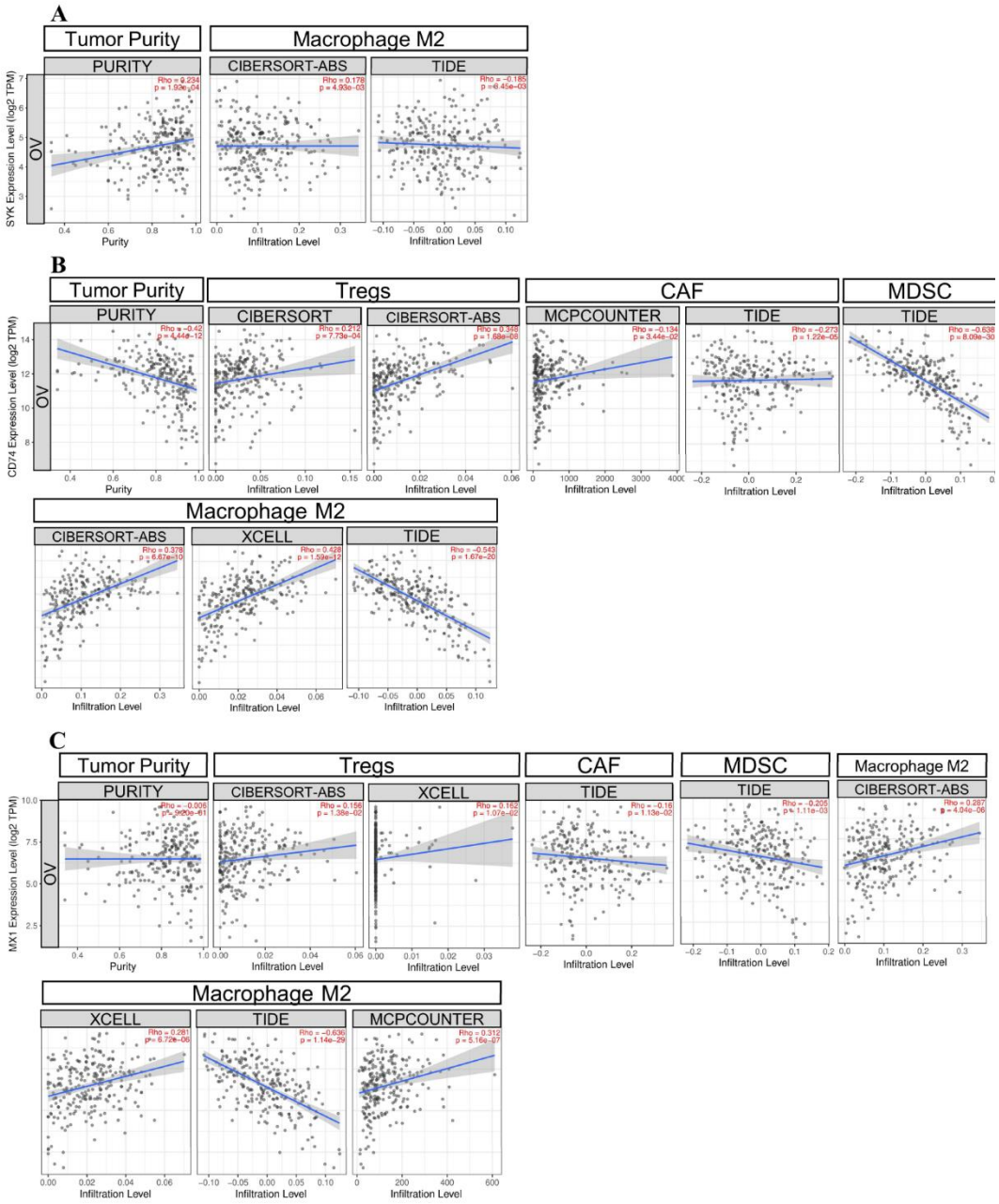

Figure S6. Association of SYK, CD74, and MX1 with immune-suppressive cell infiltration. Scatter plots show correlations between (A) SYK, (B) CD74 and (C) MX1 gene expression (log_2TPM) and estimated levels of tumor purity, Tregs, CAFs, MDSCs, and macrophage M2 across TCGA-OV tumors using representative algorithms (e.g., CIBERSORT, CIBERSORT-ABS, MCPCOUNTER, TIDE and XCELL). Blue lines indicate fitted regression; r and P values are reported in each panel.

Table S1. Biological process and MsigDB enrichment analysis of DpOCSCs-related up-and down-regulated genes

		Term	Genes
Up-regulated genes	Biological Process (BP)	Protection From Natural Killer Cell Mediated Cytotoxicity (GO:0042270)	*HLA-B; SERPINB9; HLA-G*
		C-X-C Chemokine Receptor CXCR4 Signaling Pathway (GO:0038159)	*LYN; CXCR4*
		Adiponectin-Activated Signaling Pathway (GO:0033211)	*CSNK2B; ADIPOR1*
		Interleukin-4-Mediated Signaling Pathway (GO:0035771)	*STAT5A; IL4R*
		Negative Regulation of Myeloid Leukocyte Mediated Immunity (GO:0002887)	*SPI1; CD300A*
		Negative Regulation of Toll-Like Receptor 2 Signaling Pathway (GO:0034136)	*LYN; TNFAIP3*
		Neutrophil Degranulation (GO:0043312)	*VAMP8; STXBP2*
		Regulation of Interleukin-23 Production (GO:0032667)	*RNASE1; TLR4; MYD88*
		Regulation of Myeloid Leukocyte Mediated Immunity (GO:0002886)	*LYN; SYK; STXBP2*
		Negative Regulation of Leukocyte Proliferation (GO:0070664)	*LYN; GSTP1; TNFAIP3*
	MSigDB Hallmark	Interferon Alpha Response	*IFITM3; CD74; IL4R; RSAD2; STAT2; MX1; TAP1; GMPR; IFI44; PARP14; PARP12; IFIT2; BST2; ISG20; PSME2; B2M; IRF9*
		Interferon Gamma Response	*IFITM3; CDKN1A; EIF4E3; TNFAIP3; IFIT1; IFIT2; PIM1; B2M; CD74; IL4R; RSAD2; STAT2; IL10RA; MX1; HLA-B; LYSMD2; IFI44; TAP1; HLA-A; PARP14; HLA-G; PARP12; NFKB1; BST2; VAMP8; ISG20; NFKBIA; PSME2; VAMP5; MYD88; IRF9*
		TNF-alpha Signaling via NF-kB	*STAT5A; PTGER4; PPP1R15A; CDKN1A; GADD45B; CEBPD; DUSP1; PLEK; TAP1; TNFAIP3; SLC2A3; CFLAR; LITAF; TNF; NFKB1; IFIT2; NFKBIA; KLF6; MARCKS; BHLHE40; OLR1; NFKBIE; IER5; B4GALT5*
		IL-6/JAK/STAT3 Signaling	*IL4R; IL10RB; STAT2; PIM1; CD14; TNFRSF1B; TNF; IRF9; MYD88*
		Hypoxia	*PPP1R15A; CDKN1A; DUSP1; GAA; CXCR4; TNFAIP3; SLC2A3; SLC2A5; PLAC8; TPST2; ISG20; KLF6; NAGK; XPNPEP1; BHLHE40; PIM1; MYH9; SLC37A4; FBP1; GALK1*
		Inflammatory Response	*LYN; PTGER4; CDKN1A; IL4R; SLC31A2; SEMA4D; IL10RA; AQP9; RHOG; NOD2; TNFRSF1B; NFKB1; BST2; NFKBIA; KLF6; STAB1; OLR1; CD14; MET*
		TGF-beta Signaling	*PPP1R15A; HDAC1; FURIN; RHOA; ENG*
		IL-2/STAT5 Signaling	*IFITM3; AHCY; IL4R; GADD45B; GPX4; IL10RA; CTSZ; SLC2A3; FURIN; TNFRSF1B; CCND3; MUC1; KLF6; SYNGR2; BHLHE40; SPP1; PIM1; SLC39A8*
		Complement	*LYN; FCN1; C1QA; ITGAM; GCA; PRKCD; PLEK; RHOG; WAS; TNFAIP3; LIPA; PLA2G7; XPNPEP1; PIM1; OLR1; LTA4H; CTSD; HSPA1A*
		Angiogenesis	*THBD; SPP1; OLR1*
Down-regulated	Biological Process (BP)	Fibroblast Growth Factor Receptor Signaling Pathway (GO:0008543)	*FGF7; FGF14*
		Cellular Response to Fibroblast Growth Factor Stimulus (GO:0044344)	*FGF7; FGF14*

Table S2. Cellular component and molecular function enrichment analysis of DpOCSCs-related up-and down-regulated genes

		Term	Overlap	Adjusted P-value	Genes
Up-regulated genes	Cellular Component (CC)	Tertiary Granule (GO:0070820)	24/163	1.82E-13	*ITGAM; CANT1; CD93; CD300A; IDH1; GAA; STXBP2; ITGB2; NBEAL2; SLC2A3; RNASE1; RHOA; VAMP8; CST3; NRAS; TSPAN14; OLR1; ENPP4; NCKAP1L; LTA4H; B2M; CTSD; LAIR1; ATP6V0A1*
		Ficolin-1-Rich Granule (GO:0101002)	24/184	1.48E-12	*FCN1; CANT1; CD93; CD300A; GMFG; IDH1; GAA; GSTP1; CTSZ; ITGB2; NBEAL2; SLC2A3; APEH; RNASE1; RHOA; CST3; CSNK2B; ENPP4; NCKAP1L; LTA4H; CTSD; HSPA1B; ATP6V0A1; HSPA1A*
		Secretory Granule Membrane (GO:0030667)	25/279	1.41E-09	*ITGAM; ITGB2; SLC2A3; SLC2A5; NCSTN; NRAS; PGRMC1; OLR1; NCKAP1L; ENPP4; LAIR1; ATP6V0A1; CD93; CD300A; GAA; HLA-B; RHOG; NBEAL2; LHFPL2; TNFRSF1B; RNASE1; RHOA; BST2; VAMP8; TSPAN14*
		Cytoplasmic Vesicle Membrane (GO:0030659)	30/415	2.27E-09	*COLEC12; VPS4A; DYSF; SLC2A3; ARRB2; SNX3; NCSTN; STAB1; NCKAP1L; SLC15A3; CTSD; ATP6V0A1; ATP6V1F; LYN; CD74; ATP6V0B; CD93; ATP6AP1; SORT1; HLA-B; RHOG; VPS37C; RNASE1; SORL1; RHOA; VAMP8; ATP6V0D1; TLR4; VAMP5; MYD88*
		Specific Granule (GO:0042581)	18/159	1.32E-08	*ITGAM; CANT1; CD93; STXBP2; CTSZ; ITGB2; SLC2A3; SLC2A5; TNFRSF1B; NFKB1; VAMP8; PGRMC1; TSPAN14; OLR1; HPSE; B2M; CTSD; LAIR1*
		Lysosome (GO:0005764)	32/532	3.59E-08	*IFITM3; STXBP2; CTSZ; VPS4A; CXCR4; LITAF; NCSTN; SLC39A8; ACP2; SLC15A3; B2M; CTSD; ATP6V0A1; ATP6V1F; LYN; SRGN; CD74; ATP6V0B; SLC31A2; ATP6AP1; SORT1; GAA; RNASET2; PRKCD; VAMP8; CLCN7; PPT1; SPNS1; ATP6V1B2; HPSE; ATP6V0D1; ADA*
		Phagocytic Vesicle (GO:0045335)	14/100	5.44E-08	*ATP6V0B; SYK; NCF2; HLA-B; HLA-A; NOD2; HLA-G; SNX3; VAMP8; RAB20; RAC2; ATP6V0D1; B2M; ATP6V0A1*
		Bounding Membrane of Organelle (GO:0098588)	42/881	7.33E-08	*COLEC12; CTSZ; VPS4A; SLC2A3; FURIN; ARRB2; SNX3; NCSTN; NRAS; CYTH4; STAB1; CHST15; NCKAP1L; SLC15A3; B2M; CTSD; CYTH1; ATP6V0A1; ATP6V1F; BOK; LYN; GBP5; CD74; ATP6V0B; CD93; ATP6AP1; SORT1; HLA-B; RHOG; VPS37C; HLA-A; HLA-G; RNASE1; SORL1; RHOA; VAMP8; TPST2; MGAT4A; ATP6V0D1; TLR4; MYD88; B4GALT5*
		Tertiary Granule Membrane (GO:0070821)	12/72	7.93E-08	*VAMP8; NRAS; TSPAN14; ITGAM; CD93; CD300A; GAA; ITGB2; OLR1; SLC2A3; NBEAL2; LAIR1*
		Ficolin-1-Rich Granule Membrane (GO:0101003)	11/60	1.13E-07	*CD93; CD300A; GAA; ITGB2; SLC2A3; ENPP4; NCKAP1L; NBEAL2; RNASE1; RHOA; ATP6V0A1*
	Molecular Function (MF)	Endopeptidase Regulator Activity (GO:0061135)	6/49	0.02117	*CST3; GBP5; NCSTN; PSME2; SPINT2; RENBP*
		Protease Binding (GO:0002020)	9/119	0.02117	*CST3; DERL1; TNFAIP3; FLOT2; D23A; SERPINB9; FURIN; FLAR; TNF*
		Ubiquitin-Like Protein Ligase Binding (GO:0044389)	15/284	0.02117	*DAZAP2; MOAP1; STAT2; DERL1; CXCR4; ARRB2; TNFRSF1B; NFKBIA; TUBA1B; TNFRSF14; TMBIM6; IKBKG; SLC25A5; HSPA1B; HSPA1A*
		Ubiquitin Protein Ligase Binding (GO:0031625)	14/268	0.02117	*DAZAP2; MOAP1; DERL1; CXCR4; ARRB2; TNFRSF1B; NFKBIA; TUBA1B; TNFRSF14; TMBIM6; IKBKG; SLC25A5; HSPA1B; HSPA1A*
		Protein Kinase Binding (GO:0019901)	22/527	0.02117	*PPP1R15A; DAZAP2; GSTP1; PRKCD; PLEK; ITGB2; RHOG; WAS; NBEAL2; NOD2; ADIPOR1; RNASE1; RHOA; CCND3; MAPKAPK3; ACTBL2; RAC2; SPNS1; JTB; HCLS1; CSK; EZR*
Down-regulated	Molecular Function (MF)	Fibroblast Growth Factor Receptor Binding (GO:0005104)	2/25	0.0157	*FGF7; FGF14*

Table S3. Identification of hub genes with various algorithms

Stress	Radiality	MNC	MCC	EPC	Degree	Closeness	Betweenness
SYK	SYK	SYK	SYK	SYK	SYK	SYK	SYK
NFKB1	SIGLEC1	NCF2	NCF2	SIGLEC1	SIGLEC1	SIGLEC1	NFKB1
RAC2	NCF2	SIGLEC1	SIGLEC1	NCF2	NCF2	NCF2	RAC2
ACO2	NFKB1	NFKB1	ISG20	NFKB1	NFKB1	NFKB1	ACO2
IL10RA	MAP2K1	MAP2K1	RHOG	MAP2K1	MAP2K1	MAP2K1	IL10RA
HCLS1	RAC2	RAC2	NFKB1	RAC2	RAC2	RAC2	MYH9
NRAS	IL10RA	IFI44	MAP2K1	IFI44	VAV1	IL10RA	NRAS
ATP5F1B	VAV1	VAV1	RAC2	IL10RA	IL10RA	VAV1	ATP5F1B
MYH9	HCLS1	IL10RA	HERC5	VAV1	HCLS1	HCLS1	EZR
PCBP1	MYH9	HCLS1	IFI44	HCLS1	NRAS	MYH9	PCBP1
SRSF2	VIM	RSAD2	VAV1	RSAD2	ATP5F1B	NRAS	MET
MET	MET	NRAS	IL10RA	MET	MET	VIM	VIM
VIM	SPI1	ATP5F1B	IFI6	VIM	VIM	MET	SRSF2
SPI1	PRDX1	SPI1	HCLS1	SPI1	SPI1	SPI1	SPI1
PRDX1	TNF	PRDX1	RSAD2	TNF	PRDX1	PRDX1	PRDX1
TNF	HAVCR2	TNF	SPI1	WAS	TNF	TNF	TM9SF2
HSPA1B	HSPA1B	WAS	IFITM3	HAVCR2	WAS	HAVCR2	TNF
ITGAM	PSME2	HAVCR2	TNF	HSPA1B	HAVCR2	HSPA1B	HSPA1B
C1QA	ITGAM	HSPA1B	WAS	ITGAM	HSPA1B	PSME2	ITGAM
MS4A6A	PRKCD	ITGAM	HAVCR2	PRKCD	ITGAM	ITGAM	GLUL
TLR4	HLA-G	C1QB	ITGAM	C1QB	C1QA	PRKCD	C1QA
ITGB2	C1QA	HLA-G	PRKCD	C1QA	TLR4	HLA-G	TLR4
HLA-B	TLR4	C1QA	C1QA	TLR4	ITGB2	C1QA	ITGB2
HLA-A	ITGB2	TLR4	TLR4	ITGB2	HLA-B	TLR4	HLA-B
B2M	HLA-B	ITGB2	ITGB2	HLA-B	HLA-A	ITGB2	HLA-A
MX1	HLA-A	HLA-B	FERMT3	HLA-A	IFIT1	HLA-B	B2M
B4GALT5	B2M	HLA-A	IFIT1	IFIT1	B2M	HLA-A	MX1
CXCR4	MX1	IFIT1	B2M	B2M	MX1	B2M	B4GALT5
STAT2	CXCR4	B2M	MX1	MX1	CXCR4	MX1	CXCR4
MUC1	TNFRSF1B	MX1	NCKAP1L	CXCR4	TNFRSF1B	CXCR4	MUC1
HK3	STAT2	CXCR4	CXCR4	TNFRSF1B	STAT2	TNFRSF1B	CNDP2
IDH1	MUC1	TNFRSF1B	TNFRSF1B	STAT2	MUC1	STAT2	HK3
PLCB2	IDH1	STAT2	STAT2	MUC1	IDH1	MUC1	IDH1
ARRB2	STAT5A	MUC1	STAT5A	STAT5A	STAT5A	IDH1	PLCB2
SPP1	ARRB2	IDH1	IKBKG	SPP1	SPP1	STAT5A	ARRB2
ADA	SPP1	STAT5A	GBP5	IKBKG	GBP5	SPP1	SPP1
ITGB4	IKBKG	SPP1	MYD88	MYD88	MYD88	IKBKG	ADA
MYD88	MYD88	MYD88	PARP14	LYN	LYN	MYD88	ITGB4
PARP14	LYN	LYN	LYN	NFKBIA	NFKBIA	LYN	GBP5
NFKBIA	NFKBIA	NFKBIA	NFKBIA	IRF9	IRF9	NFKBIA	NFKBIA
IRF9	IRF9	IRF9	IRF9	CDKN1A	CDKN1A	IRF9	HDAC1
HDAC1	CDKN1A	CDKN1A	PARVG	HDAC1	HDAC1	CDKN1A	BCAP31
BCAP31	HDAC1	HDAC1	TNFAIP3	TNFAIP3	TNFAIP3	HDAC1	CTSD
CTSD	TNFAIP3	TNFAIP3	CD74	DUSP1	CTSD	TNFAIP3	GLA
GLA	CTSD	CD74	BST2	CD74	CD74	CTSD	GPX4
FCN1	MAPK13	BST2	RHOA	RHOA	RHOA	CD74	SORT1
CD74	CD74	RHOA	IFIT2	BST2	BST2	RHOA	CD74
RHOA	RHOA	IFIT2	PLEK	IFIT2	IFIT2	BST2	ESYT1
IFIT2	NOD2	PLEK	NOD2	PLEK	PLEK	NOD2	RHOA
PLEK	PLEK	NOD2	PARP12	NOD2	NOD2	PLEK	PLEK

Table S4. Analysis of complementarity in interactions among DpOCSC-related hub genes

Gene symbol	Betweenness	Closeness	Degree	EcCentricity	Radiality	Stress
SYK	1190.4523	0.0014	37	0.2	5.5877	17452
NFKB1	3180.1503	0.0015	54	0.2	5.7577	42288
RAC2	1800.1874	0.0014	31	0.2	5.5237	20342
IL10RA	1120.4681	0.0013	29	0.2	5.4624	13382
SPI1	2299.3364	0.0014	39	0.2	5.5627	25276
TNF	22801.8213	0.0018	99	0.25	5.9749	157962
ITGAM	3146.6946	0.0014	52	0.2	5.6351	30564
C1QA	1470.3774	0.0013	27	0.2	5.4902	12780
TLR4	3563.332	0.0015	62	0.2	5.7298	40644
ITGB2	3480.6403	0.0014	50	0.2	5.6044	38404
B2M	3822.7107	0.0014	41	0.2	5.6212	34396
MX1	2307.2987	0.0014	32	0.2	5.5125	24898
CXCR4	1359.4886	0.0015	40	0.2	5.6462	16292
NFKBIA	2805.2703	0.0015	46	0.2	5.688	28614
CD74	3586.2192	0.0015	35	0.2	5.6546	34750
RHOA	7648.8837	0.0015	47	0.2	5.7242	52436
PLEK	2567.7044	0.0014	32	0.2	5.5125	19780
Whole network average	4008.8845	0.0014	44.2941	0.2029	5.6287	35897.647

Table S5. Gene ontologies (GO) enrichment analysis of DpOCSCs-associated hub genes

	Term	Overlap	Adjusted P-value	Genes
Biological Process (BP)	Macrophage Activation (GO:0042116)	6/37	2.32E-10	*C1QA; ITGAM; SYK; ITGB2; TNF; TLR4*
	Regulation of Neutrophil Degranulation (GO:0043313)	4/5	6.49E-10	*ITGAM; SPI1; SYK; ITGB2*
	Cytokine-mediated Signaling Pathway (GO:0019221)	7/287	4.86E-07	*NFKBIA; SPI1; SYK; IL10RA; MX1; TNF; NFKB1*
	Positive Regulation of Chemokine (C-X-C Motif) Ligand 2 Production (GO:2000343)	3/8	2.96E-06	*CD74; TLR4; TNF*
	Regulation of Canonical NF-kappaB Signal Transduction (GO:0043122)	6/301	6.66E-06	*NFKBIA; CD74; SPI1; TNF; TLR4; RHOA*
	Positive Regulation of Chemokine Production (GO:0032722)	4/57	7.04E-06	*CD74; SYK; TNF; TLR4*
	Regulation of Chemokine (C-X-C Motif) Ligand 2 Production (GO:2000341)	3/14	7.90E-06	*CD74; TNF; TLR4*
	Positive Regulation of Interleukin-8 Production (GO:0032757)	4/65	8.97E-06	*CD74; SYK; TNF; TLR4*
	Regulation of Cytokine Production Involved in Inflammatory Response (GO:1900015)	4/65	8.97E-06	*NFKBIA; TNF; TLR4; NFKB1*
	Positive Regulation of Interleukin-6 Production (GO:0032755)	4/78	1.55E-05	*CD74; SYK; TNF; TLR4*
Cellular Component (CC)	Specific Granule (GO:0042581)	4/159	3.49E-04	*ITGAM; ITGB2; B2M; NFKB1*
	Tertiary Granule (GO:0070820)	4/163	3.49E-04	*ITGAM; ITGB2; B2M; RHOA*
	Phagocytic Vesicle (GO:0045335)	3/100	0.00196	*SYK; RAC2; B2M*
	Focal Adhesion (GO:0005925)	4/387	0.0041	*ITGB2; RAC2; B2M; RHOA*
	Cell-Substrate Junction (GO:0030055)	4/395	0.0041	*ITGB2; RAC2; B2M; RHOA*
	Endocytic Vesicle Membrane (GO:0030666)	3/165	0.0041	*CD74; RAC2; B2M*
	Membrane Raft (GO:0045121)	3/171	0.0041	*ITGAM; ITGB2; TNF*
	Phagocytic Vesicle Membrane (GO:0030670)	2/48	0.0065	*RAC2; B2M*
	Late Endosome (GO:0005770)	3/222	0.0065	*CD74; CXCR4; B2M*
	ER to Golgi Transport Vesicle Membrane (GO:0012507)	2/54	0.0065	*CD74; B2M*
Molecular Function (MF)	Complement Component C3b Binding (GO:0001851)	2/10	0.0018	*ITGAM; ITGB2*
	MHC Class II Protein Complex Binding (GO:0023026)	2/24	0.0055	*CD74; B2M*
	Protein Kinase Binding (GO:0019901)	4/527	0.0148	*ITGB2; PLEK; RAC2; RHOA*
	Myosin Binding (GO:0017022)	2/57	0.0148	*CXCR4; RHOA*
	GTPase Activity (GO:0003924)	3/266	0.0148	*MX1; RAC2; RHOA*
	Ribonucleoside Triphosphate Phosphatase Activity (GO:0017111)	3/274	0.0148	*MX1; RAC2; RHOA*
	Cytokine Receptor Activity (GO:0004896)	2/83	0.0187	*CD74; IL10RA*
	MHC Class II Protein Binding (GO:0042289)	1/5	0.0313	*CD74*
	CD4 Receptor Binding (GO:0042609)	1/7	0.0372	*CD74*
	STAT Family Protein Binding (GO:0097677)	1/8	0.0372	*SPI1*

Table S6. Relevance of non-supported DpOCSC-related hub genes to clinico-pathological

Clinical significance	Hub genes
Lymphatic invasion[a]	*TLR4***, *B2M****, *ITGAM****, *NFKBIA**
Venous invasion[a]	*TLR4**, *B2M**, *ITGAM**, *NFKBIA****
Primary therapy outcome success[b]	*RHOA**

a: Yes/No; d: Partial remission/ Stable disease/ Progressive disease/Complete remission. (* = $P < 0.05$, ** = $P < 0.01$, *** = $P < 0.001$, **** = $P < 0.0001$) (NFKB1 was excluded from the analysis due to the lack of an inappropriate cut-off point)

Table S7. Signaling pathways associated with non-supported hub genes associated with DpOCSCs

Signaling pathways	Platform	Hub genes
Wnt/β-catenin/TCF/LEF	TRUST 2019	*TLR4* (TCF, TCF); *NFKB1* (TCF4); *IL10RA* (TCF3, LEF1)
	TRANSFAC and JASPAR	*B2M* (TCF4); *ITGAM* (LEF1, TCF4); *NFKBIA* (TCF4); *NFKB1* (TCF4)
STAT3	JASPAR PWM human 2025	*NFKB1* (STAT3)
TGFβ/Smad2/3/4	ChEA 2022 and ChIP-seq 2015	*NFKB1* (SMAD4 in A2780); *IL10RA* (SMAD4 in A2780)
	JASPAR PWM human 2025	*IL10RA* (SMAD2)
NFκB	TRUST 2019	*B2M* (NFKB1); *NFKBIA* (NFKB1); *NFKB1*(NFKB1)
	TRANSFAC and JASPAR	*NFKBIA* (NFKB1); *NFKB1* (NFKB1)
	JASPAR PWM human 2025	*IL10RA* (NFKB1, NFKB2)
Notch	JASPAR PWM human 2025	*NFKB1* (RBPJ)
Hippo-YAP1/TAZ-TEAD	JASPAR PWM human 2025	*RHOA* (TEAD1); *TLR4* (TEAD1); *ITGAM* (TEAD1); *NFKB1* (TEAD1-4);

A2780: ovarian cancer from untreated patient